THE ASTRONOMICAL JOURNAL, 117:937–961, 1999 February

MULTICOLOR CCD PHOTOMETRY AND STELLAR EVOLUTIONARY ANALYSIS OF NGC 1907, NGC 1912, NGC 2383, NGC 2384, AND NGC 6709 USING SYNTHETIC COLOR-MAGNITUDE DIAGRAMS

ANNAPURNI SUBRAMANIAM
Indian Institute of Astrophysics, Koramangala, Bangalore 560 034, India; purni@iiap.ernet.in

AND

RAM SAGAR
Indian Institute of Astrophysics, Bangalore 560 034, India; and Uttar Pradesh State Observatory, Manora Peak, Nainital 263 129, India; sagar@upso.ernet.in

Received 1996 October 9; accepted 1998 September 14

ABSTRACT

We present the first CCD photometric observations of NGC 2383 and NGC 2384 in B, V, R, and I, NGC 1912, NGC 6709 in B, V, and I and NGC 1907 in B and V passbands, reaching down to a limiting magnitude of $V \sim 20$ mag for ~ 3300 stars put together. The results of the spectroscopic observations of 43 bright stars in the field of NGC 1912, NGC 2383, NGC 2384, and NGC 6709 are also presented. The color-magnitude diagrams (CMDs) of the clusters in V versus $B-V$, V versus $V-R$, and V versus $V-I$ are presented. The distances and reddening to these clusters are determined using the cluster CMDs. The distances to the clusters NGC 1907, NGC 1912, NGC 2383, NGC 2384, and NGC 6709 are 1785 ± 260, 1820 ± 265, 3340 ± 490, 2925 ± 430, and 1190 ± 175 pc, respectively. Some gaps in the cluster main sequence have been identified. We have compared the observed color-magnitude diagrams of these four open clusters with the synthetic ones derived from one classical and two overshoot stellar evolutionary models. Overshoot models estimate older ages for clusters when compared to the classical models. The age of the clusters estimated using the isochrones of Bertelli et al. are 400, 250, 400, 20, and 315 Myr for the clusters NGC 1907, NGC 1912, NGC 2383, NGC 2384, and NGC 6709, respectively. A comparison of the synthetic color-magnitude diagrams with the observed ones indicates that the overshoot models should be preferred. The comparison of integrated luminosity functions do not clearly indicate as to which model is to be preferred. The values of the mass function slopes estimated for the clusters are $x = 1.7 \pm 0.15$ for NGC 1912 (mass range: 1.7–3.9 $M_\odot$) and NGC 6709 (1.7–3.4 $M_\odot$), $x = 1.3 \pm 0.15$ for NGC 2383 (1.7–3.1 $M_\odot$), and $x = 1.0 \pm 0.15$ for NGC 2384 (2.0–14.0). The present age estimates show that the closely located cluster pair NGC 1912 + NGC 1907 have similar ages, indicating that they may have born together, making them a good candidate to be a binary open cluster.

Key words: open clusters and associations: general — open clusters and associations: individual (NGC 1907, NGC 1912, NGC 2383, NGC 2384, NGC 6709) — stars: evolution — stars: luminosity function, mass function

1. INTRODUCTION

The open star clusters have been the focus of investigation, for various reasons, from the early part of this century. Though there are about 1400 open star clusters known in our Galaxy, the clusters whose distances are known only number about 400 (Lyngå 1987), and the other cluster parameters like age and reddening are in a similar state. Also, most of the clusters are studied through photoelectric or photographic photometry, which are less accurate and limited to brighter magnitudes. The color-magnitude diagrams (CMDs) thus obtained terminate at relatively large brightness levels, and hence the evolutionary features may not be brought out properly, especially in the case of intermediate-age and old clusters. Thus, a deeper and systematic study of Galactic open clusters is attempted here.

The aim of the study is to acquire a set of homogeneous data on open clusters to derive their parameters, such as distance, reddening, and age. We have used these parameters to understand the clusters individually. These data help us to estimate the power law of the mass function in the clusters studied here. Another aim of this study is to compare the observational CMDs of open star clusters of our Galaxy with the stellar evolutionary models in order to identify the input physical mechanisms responsible for the observed features in the cluster CMDs. In order to compare the CMDs of open clusters with those from the stellar models, the richness of the cluster is important as we need the stars to be populated in various evolutionary stages. Therefore, to identify the observational features sensitive to the core overshooting in the CMDs of star clusters, the turn-off masses of stars should lie in the mass range 1.5–10 $M_\odot$. The effects of core overshoot are difficult to identify in stars with masses less than 1.5 $M_\odot$, due to their very small cores, and stars with masses above 10 $M_\odot$ lose mass in the MS itself, making a direct comparison between the observation and theory difficult. Very young clusters (age $\leq 10^7$ yr) have the problems of low-mass stars still in the pre-MS phase and the presence of differential reddening across the cluster. The old clusters (age $\geq 10^9$ yr) have dynamical relaxation times smaller than their ages and hence would have lost significant number of low-mass stars due to relaxation. The intermediate-age clusters (age around 10^8 yr) would not have relaxed dynamically and are not generally seen to have differential reddening.

The evolutionary studies of many open clusters have been attempted to identify the presence of the core over-

shoot and to identify the efficiency of mixing. While analyzing clusters like the Pleiades, Maeder & Mermilliod (1981) noticed that the main sequence (MS) extends to too bright a luminosity to fit standard models and suggested a certain amount of overshoot in the core. There are also many similar recent works on old open clusters with turn-off mass less than 2 $M_\odot$ (Aparicio et al. 1990; Anthony-Twarog et al. 1991; Bergbusch, VandenBerg, & Infante 1991; Aparicio et al. 1993). The study by Castellani, Chieffi, & Straniero (1992) on the CMDs of Hyades, Pleiades, Praesepe, NGC 2420, NGC 3680, and NGC 188 with the aid of classical models found that if the new opacity, as in the Los Alamos Opacity Library of Huebner et al. (1977), is used, there is no need for the overshoot of the convective core. The studies of Aparicio et al. (1990) and Bertelli, Bressan, & Chiosi (1992) found that the models with overshoot for stars in the mass range 1.5–2 $M_\odot$ as calculated by Bertelli et al. (1986a, 1986b) overestimated the overshoot distance, whereas those by Maeder & Meynet (1989, 1991), calculated with a moderate amount of core overshoot, suffered from an inconsistency in the evaluation of the stellar lifetime. On the other hand, they suggested that a certain amount of overshoot is always required. In the case of old open clusters, both classical and overshoot models can lead to a reasonable fit to the CMDs as shown by Bertelli et al. (1993) and Carraro et al. (1994). However, looking at both the CMD and luminosity function (LF), several differences between the classical and overshoot models can be noticed (Alongi et al. 1993). Therefore, the question regarding the need for the inclusion of core overshoot in stellar models is still open.

The open clusters are the product of the star formation activity in the Galactic disk. One or more clusters are formed as a result of the star formation activity in a molecular cloud. These clusters may or may not stay together for a long time due to their individual velocity dispersion and also due to the Galactic tidal force. Subramaniam et al. (1995) noticed a few cluster pairs with separation less than 20 pc among the open clusters. We have included two such pairs in this study to redetermine their parameters including distance, to estimate their closeness. We plan to test their candidacy for double cluster. The age estimation will tell us whether they are born at the same time and hence presumably from the same molecular cloud. The pairs are NGC 1907 + NGC 1912 and NGC 2383 + NGC 2384. The clusters chosen for the present study are NGC 1907, NGC 1912, NGC 2383, NGC 2384, and NGC 6709.

2. EARLIER STUDIES

The parameters of the five clusters as cataloged in Lyngå (1987) are given in Table 1. Earlier studies of the individual clusters are discussed below.

NGC 1907.—This cluster is situated close to NGC 1912, in Auriga, and its Trumpler class is I 1 m. Trumpler (1930) found a distance of 2750 pc, Collinder (1931) found it to be 4750 pc, and Becker (1963) obtained 1380 pc as the distance. The U, B, and V photoelectric photometry of 27 stars and photographic photometry of 24 stars are available from Hoag et al. (1961). Hoag (1966) found a distance of 1380 pc and $E(B-V)$ of 0.38 mag, but Hoag & Applequist (1965) found the distance as 1200 pc and the same reddening. Hoag (1966) found that the distance modulus ranged from 10.4 to 11.2 mag. Strobel (1991) found that the cluster has a metallicity [M/H] = −0.20. The radial velocity of eight stars were determined by Glushkova & Rastorguev (1991).

NGC 1912.—This is an open cluster situated in the anticenter direction of the Galaxy, and its Trumpler classification is II 2 r. Johnson (1961) estimated the distance to be 1320 pc and the reddening, $E(B-V)$, to be 0.27 mag. Becker (1963) found the distance and $E(B-V)$ as 1415 pc and 0.24 mag, respectively. The detailed photometric study was done by Hoag et al. (1961), where photoelectric photometry of 28 stars and photographic photometry of 137 stars were obtained in U, B, and V passbands. The follow-up paper by Hoag & Applequist (1965) found 870 pc and 0.27 mag as the distance and the $E(B-V)$ values, respectively. A wide range in the distance moduli (8.7–10.6 mag) was found for the stars in this cluster by Hoag (1966). There is proper motion information available for about 383 stars (Mills 1967). Spectroscopic information is available only for a few stars in this cluster (Hoag & Applequist 1965; Hiltner 1956; Sowell 1987) and the radial velocity of seven stars were determined by Glushkova & Rastorguev (1991). Sears & Sowell (1997) have recently done the spectral classification of 10 stars in the cluster.

NGC 2383.—This is a compact and moderately rich cluster in the constellation of Canis Major and the Trum-

TABLE 1

BASIC CLUSTER PARAMETERS OF THE FIVE OPEN CLUSTER AS GIVEN THE CATALOG OF LYNGÅ 1987

PARAMETER	VALUE				
	NGC 1907	NGC 1912	NGC 2383	NGC 2384	NGC 6709
R.A. (1950.0)	5 24.7	5 25.3	7 22.6	7 22.9	18 49.1
Decl. (1950.0)	+35 17	+35 48	−20 50	−20 56	+10 17
Galactic longitude (deg)	1720.62	1720.27	2350.26	2350.39	420.16
Galactic latitude (deg)	0.30	0.70	−2.44	−2.41	4.70
Trumpler class	I 1 m n	II 2 r	II 3 m	IV 3 p	IV 2 m
Ang. diameter (arcmin)	5.0	14	5.0	5.0	14
Distance (pc)	1380	1320	2000	2000	950
$E(B-V)$ (mag)	0.42v	0.24	0.27	0.29	0.30
log (age)	8.64	8.35	7.40	6.00	7.89
[Fe/H]	−0.10	−0.11	...	...	...
Radial velocity (km s^{-1})	...	...	...	31	−13
Number of peculiar member stars	...	...	...	...	1 Be star
Galactic R and z (pc)	9820; 6	9720; 15	9750; −83	9690; −137	7860; 72
Linear diameter (pc)	2.8	8.1	3.5	1.5	3.7

NOTE.—Units of right ascension are hours and minutes, and units of declination are degrees and arcminutes.

TABLE 2

LOG OF PHOTOMETRIC AND SPECTROSCOPIC OBSERVATIONS

PHOTOMETRY				SPECTROSCOPY		
Date	Telescope	Clusters	Regions	Date	Cluster	Number of Stars
1992 Feb 11	1.02 m	NGC 1912	3	1992 Feb 14	NGC 1912	8
1992 Mar 9	1.02 m	NGC 1912	3	1992 Dec 18	NGC 1912	3
1992 Mar 10	1.02 m	NGC 1912	2	1993 Feb 18	NGC 1912	6
1992 Dec 28	1.02 m	NGC 1912	2	1993 Apr 17	NGC 6709	4
1992 Dec 29	1.02 m	NGC 1912	4	1993 Apr 18	NGC 1912	1
1992 Dec 30	1.02 m	NGC 1907	2	1993 Apr 26	NGC 6709	4
1993 Jan 20	1.02 m	NGC 1907	4	1993 Jun 26	NGC 6709	7
1993 Jan 21	1.02 m	NGC 1907	2	1994 Jan 20	NGC 2383	3
1993 Feb 23	1.02 m	NGC 1912	1	1994 Feb 6	NGC 2383	7
		NGC 2383	1	1994 Feb 5	NGC 2384	4
1993 Feb 24	1.02 m	NGC 1912	1	1994 Jun 4	NGC 6709	2
		NGC 2383	1	1994 Jun 26	NGC 6709	1
1993 Mar 19	1.02 m	NGC 2383	3			
		NGC 6709	1			
1993 Mar 20	1.02 m	NGC 2383	1			
1993 May 23	1.02 m	NGC 6709	1			
1993 May 24	1.02 m	NGC 6709	4			
1993 Jun 17	1.02 m	NGC 6709	4			
1993 Jun 18	1.02 m	NGC 6709	5			
1994 Jan 15	1.02 m	NGC 1907	3			
1994 Mar 19	1.02 m	NGC 6709	2			
1994 Mar 21	1.02 m	NGC 6709	2			
1994 Apr 12	1.02 m	NGC 2383	1			
1992 Mar 6	2.34 m	NGC 1912	2			
1992 Mar 7	2.34 m	NGC 1912	1			
1993 Apr 20	2.34 m	NGC 6709	3			
1994 Feb 13	2.34 m	NGC 1912	1			
1994 Feb 14	2.34 m	NGC 1912	2			
1996 Jan 13	2.34 m	NGC 2383	1			
1996 Jan 13	2.34 m	NGC 2384	1			

pler class is II 3 m. To the southeast of this cluster, another star cluster is seen, which is identified as NGC 2384. The proximity of these two clusters in the plane of the sky encourages us to find whether these two are located at the same place in the Galaxy or just a projection effect as indicated by Vogt & Moffat (1972). NGC 2383 is a very poorly studied cluster. The only single photometric study was done by Vogt & Moffat (1972), where the photoelectric photometry in U, B, and V passbands is available for 11 stars in the cluster field. They estimated the reddening, $E(B-V)$, and distance to the cluster as 0.27 mag and 1.97 kpc, respectively. Spectral information of three stars is available in Fitzgerald et. al. (1979).

NGC 2384.—This cluster lies within 5′ from NGC 2383 and is classified as IV 3 p. The earliest study of this cluster was by Trumpler (1930), and he found the distance as 2.6 kpc. Collinder (1931) found the distance to the cluster to be 4.55–4.75 kpc. The photometric study by Vogt & Moffat (1972) obtained photoelectric measurements of 15 stars in the U, B, and V passbands. They found a distance of 3.28 kpc and $E(B-V)$ of 0.29 mag. Babu (1985) obtained photoelectric photometry in the V passband for 20 stars and spectral types of 18 stars from objective grating spectra. The photographic study was done by Hassan (1984), where 49 stars were observed in the U, B, and V passbands.

NGC 6709.—This is a moderately rich cluster situated toward the center of the Galaxy and lies in the constellation of Aquila. Trumpler classifies this cluster as IV 2 m. The cluster has received a lot of attention in the early part of the century. Among the more recent studies, Johnson (1961) found a distance of 910 pc and $E(B-V)$ value of 0.30 mag. The study by Becker (1963) estimated a distance of 930 pc and $E(B-V)$ of 0.34 mag. Hoag et al. (1961) determined photoelectric photometry of 30 stars and photographic photometry of 80 stars in U, B, and V passbands. Hoag & Applequist (1965) found a value of 9.8–10.2 mag for the distance modulus. The proper motion probabilities of around 500 stars in the cluster field are available from Hakkila, Sanders, & Schroder (1983). Spectroscopic studies have shown that this cluster contains two Be stars (Schild & Romanishin 1976), and one of them was found to be a shell star (Sowell 1987). Sears & Sowell (1997) has recently done the spectral classification of eight stars in the cluster.

It can be seen that these clusters have only photographic or photoelectric data available for the bright stars in the cluster. The CCD observations of these clusters are carried out to render CMDs with better photometric accuracy and MS extending up to fainter magnitudes. These help in the precise determination of cluster parameters and to yield a good CMD for comparison with stellar models.

3. OBSERVATIONS

The clusters were observed with the 1.02 and 2.34 m telescopes at the Vainu Bappu Observatory, situated in Kavalur (India). At the Cassegrain focus (f/13) of 1.02 m Carl-Ziess reflector, CSF TH 7882 CCD chip, with a size of 384×576 pixel^2 covering 2.28×3.43 arcmin^2 of the sky was used. At the prime focus (f/3.23) of the 2.34 m Vainu

Bappu Telescope, GEC P8602 CCD chip with a size of 385×578 pixel^2 and a sky coverage of 4.0×6.1 arcmin^2 and TH 1024AB2 CCD chip of size 1024×1024 pixel^2 and 10.75×10.75 arcmin^2 sky coverage were used.

The low-resolution spectra of some bright members of four clusters (except NGC 1907) were observed using the 1.02 m telescope using the Carl-Ziess Universal Astronomical Spectrograph (UAGS) with 150 lines mm^{-1} grating giving a dispersion of 6 Å pixel^{-1} and a net resolution of 9 Å pixel^{-1} and CCD as detector. The spectrophotometric standards (Breger 1976) closer to the cluster were observed in all nights. The iron-argon spectra were used for wavelength calibration. The standard IRAF routines were used to reduce the data. The log of both photometric and spectroscopic observations are given in Table 2. The observations spanned a period of 4 years, from 1992 February to 1998 January. The typical exposure times ranged from 2 to 15 minutes, in the case of photometry, and 20 to 30 minutes in the case of spectroscopy.

During each observing run, the flats were acquired in all of the filters both in the evening and morning twilights. The bias frames were obtained at regular intervals. The bias frame closer to the observed image was used for bias subtraction. The flat frames were first bias-subtracted and trimmed before stacking (using median) to obtain master flats for each filter. These master flats are used to flat-field the images. All photometric reductions were done using the DAOPHOT II profile-fitting software (Stetson 1992). Further processing and conversion of raw instrumental magnitudes to the standard photometric system were performed using the procedure outlined by Stetson (1992). The standard stars observed are the stars in the dipper asterism region of M67 (NGC 2682). The usefulness of this region in M67 in calibrating CCDs has been discussed by several authors (Schild 1983; Sagar & Pati 1989; Joner & Taylor 1990; Chevalier & Ilovaisky 1991; Montgomery, Marschall, & Janes 1993). This region contains 16 stars within a magnitude range of 9.7 to 14 mag in V and -0.09 to 1.35 mag in $B-V$. It was observed in all filters at different air mass to obtain a reliable estimate of the atmospheric extinction coefficients. The brightest two stars in the frame are used for this purpose. Ten stars in the region were used to estimate the zero points and the color coefficients. The magnitudes and colors of standard stars were taken from Chevalier & Ilovaisky (1991). The transformation equations to the standard system are of the form

$$B_{\rm std} = b_{\rm inst} + 7.614 + 0.348(B-V)_{\rm std} + 0.685X + 0.036X(B-V)_{\rm std} ,$$

$$V_{\rm std} = v_{\rm inst} + 7.071 + 0.037(V-I)_{\rm std} + 0.540X ,$$

$$R_{\rm std} = r_{\rm inst} + 6.755 + 0.027(V-R)_{\rm std} + 0.408X ,$$

$$I_{\rm std} = i_{\rm inst} + 7.334 + 0.007(V-I)_{\rm std} + 0.295X ,$$

where "std" stands for the standard magnitudes and "inst" stands for the instrumental magnitudes. The values of the coefficients are for 1992 March 9. The open clusters in this program were observed on nonphotometric nights as well. The regions that were calibrated on a photometric night were then used to transform the rest of the cluster stars. The regions having the direct overlap are transferred to the coordinates of the calibrated frame. The stars that are in common are used to find the zero-point shift, and the stars in the overlapping region were transferred to the standard system. This method is extended to cover the entire field. The zero-point errors for the cluster stars are uncertain by ~ 0.01 mag in the B, V, R, and I filters. This included the frame-to-frame scatter and errors in the color transformation.

4. PHOTOMETRY

The observed fields of the cluster region are presented here. The figures show the X-Y plots denoting the pixel numbers, where 1 pixel corresponds to 0.″36. The photometry of 221 stars in the B and V passbands were obtained in the case of NGC 1907. The V and $B-V$ magnitudes from Hoag et al. (1961) were used to convert the present data to the standard system. The field of NGC 1907 is shown in Figure 1. All of the stars observed are shown in the V, $B-V$ CMD in Figure 2.

For NGC 1912, we have obtained photometry for ~ 740 stars in the field of NGC 1912 in B, V, and I passbands. We have obtained 140 frames in 22 overlapping regions of the cluster. The identified stars are plotted in Figure 3. As the photoelectric and the photographic data (Hoag et al. 1961), are available in V mag and in $B-V$ color, we compared our photometry with these data, as shown in Figure 4. The difference was calculated as the Hoag et al. (1961) data subtracted from the present data and the mean values and standard deviations of the differences in V and $B-V$ are -0.02 ± 0.005 and 0.01 ± 0.005, respectively. This shows that present photometry agrees well with that of Hoag et al. (1961). All stars observed are shown in the V, $B-V$ and V, $V-I$ CMDs in Figure 5.

The photometric measurements in B, V, R, and I passbands for 722 stars in the field of NGC 2383 was obtained. The X-Y plot of the stars observed are plotted in Figure 6. We identified the 11 stars observed by Vogt & Moffat (1972)

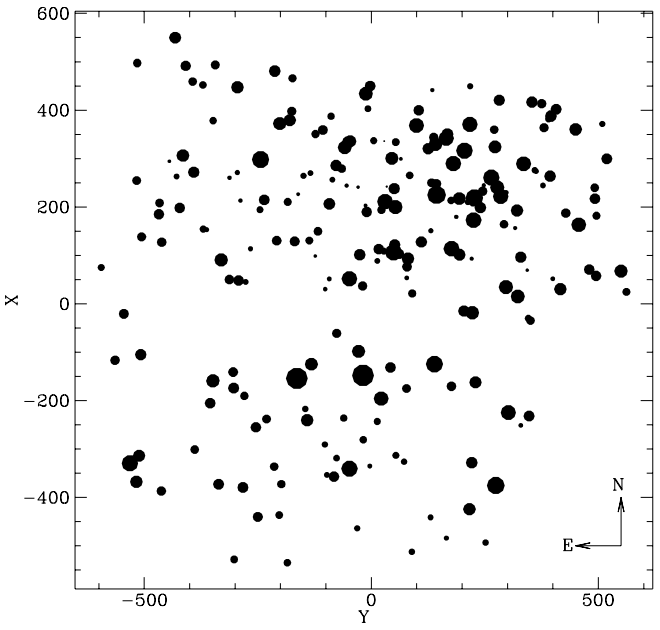

FIG. 1.—Stars observed in the cluster region of NGC 1907 are shown in the X-Y plot. The coordinates are interchanged to get north toward up and east toward the left. The size of the circle is proportional to the magnitude such that brighter the star, the bigger the circle. The X- and Y-axes are in pixels, and 1 pixel corresponds to 0.″36.

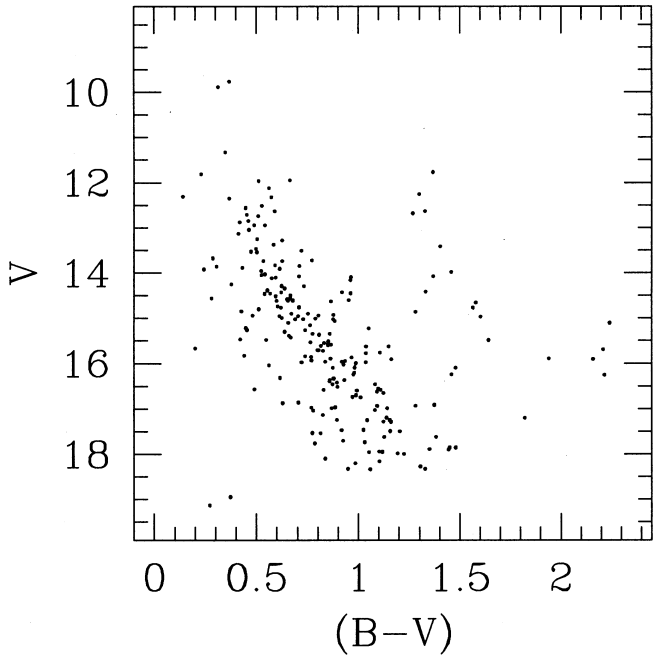

FIG. 2.—V vs. $B-V$ CMD of NGC 1907 is shown here; the number of stars present is 221.

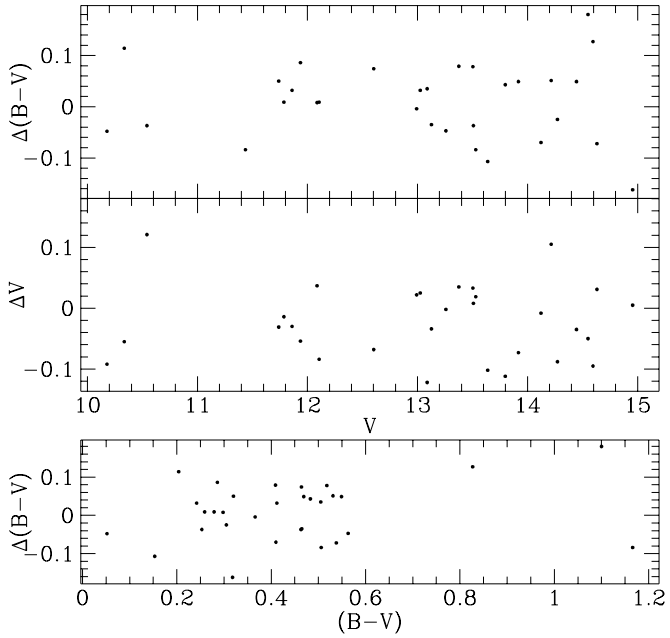

FIG. 4.—Present data of NGC 1912 are compared with the photographic data by Hoag et al. (1961). The difference in magnitudes and colors is taken as Δ = present—Hoag et al. (1961).

and compared with our photometry, as shown in Figure 7. The mean values and standard deviation of the differences in V and $B-V$ between the present data and those from Vogt & Moffat (1972) are -0.04 ± 0.009 and -0.03 ± 0.003, respectively. The data are in good agreement, except in one case where the difference is more. This is star number 6 in Vogt & Moffat (1972). We have found three stars near this star within a radius of 8″.5. The integrated magnitude of all four stars put together is 13.34 mag, still 0.09 mag fainter than the Vogt & Moffat (1972) determination. All stars observed are shown in the V versus $B-V$, V versus $V-R$, and V versus $V-I$ CMDs in Figure 8.

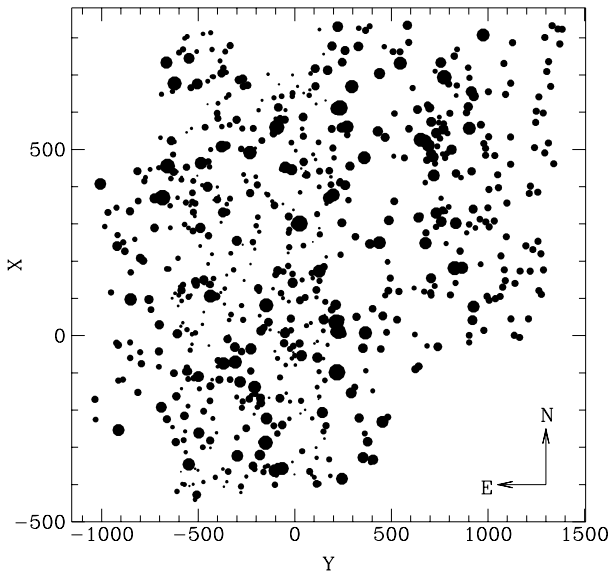

FIG. 3.—Stars observed in the cluster field of NGC 1912 are shown here.

We have obtained photometry of 304 stars in the field of NGC 2384 in B, V, R, and I passbands. The field observed for this cluster covers this cluster and part of NGC 2383. The stars in NGC 2383 were used as standard stars to transfer the stars of NGC 2384 to the standard system. The cluster region observed is shown in Figure 9. The common stars with the photometry of Vogt & Moffat (1972) and Hassan (1984) were identified and compared as in Figure 10. The mean values and standard deviations of the differences in V and $B-V$ between the present data and Vogt & Moffat (1972) data are -0.06 ± 0.002 and 0.05 ± 0.001, respectively, and in the case of the present data and Hassan (1984) the values are -0.03 ± 0.004 and 0.002 ± 0.005, respectively. The present data are in good agreement with both the earlier photometries. All stars observed are shown in the V versus $B-V$, V versus $V-R$, and V versus $V-I$ CMDs in Figure 11.

A Galactic field region near the clusters NGC 2383 and NGC 2384 was also observed. This region is approximately 5′ away from the two clusters, and we consider this region as the Galactic field for both the clusters.

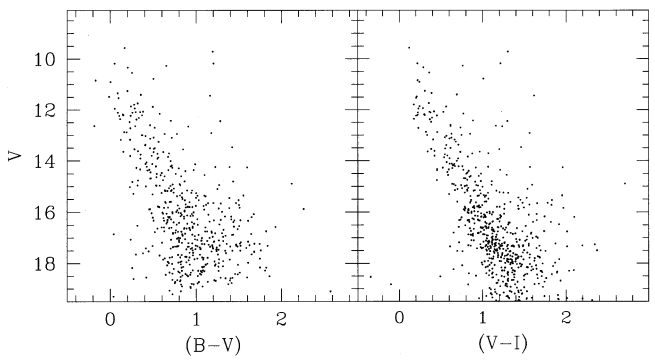

FIG. 5.—Cluster CMDs in the V vs. $B-V$ and V vs. $V-I$ planes are shown for the cluster NGC 1912.

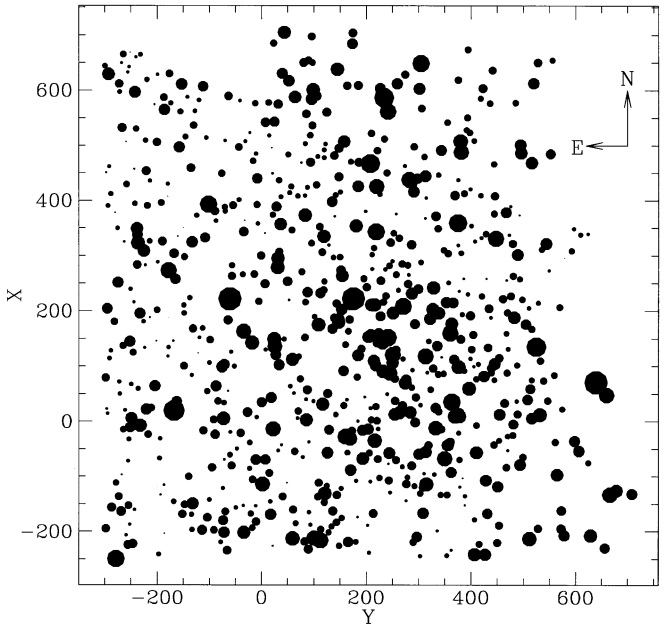

FIG. 6.—Stars observed in the field of NGC 2383 are shown here

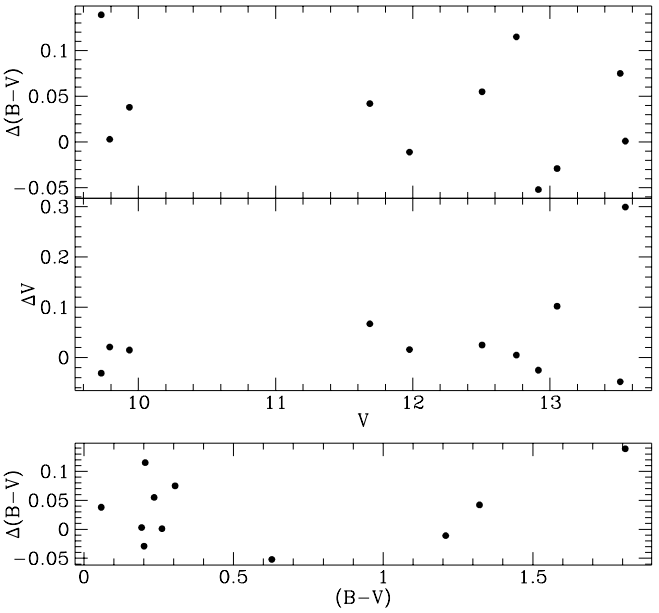

FIG. 7.—Data for NGC 2383 are compared with Vogt & Moffat (1972) for the 11 common stars. The abscissa is the present data, and the difference is calculated as Δ = present—Vogt & Moffat (1972).

In the case of NGC 6709, we have observed 1338 stars, which consisted of 22 overlapping cluster regions in 81 CCD frames in *B*, *V*, and *I* filters. All the frames were merged together to get the final cluster region, as shown in Figure 12. The present data have 10 stars in common with the photoelectric data and 23 stars in common with the photographic data of Hoag et al. (1961), and the data were compared as shown in Figure 13. The photometric magnitudes of Hoag et al. (1961) were subtracted from the present values for the comparison, and the mean and standard deviation of the differences in V and $B-V$ are 0.05 ± 0.003 and -0.05 ± 0.005, respectively. This shows that the data agree in general and no systematic trend is seen. All stars observed are shown in the V, $B-V$ and V, $V-I$ CMDs in Figure 14.

Photometric errors and data completeness.—The photometric errors were found by the method of artificial adding of stars and this is done using the routine ADDSTAR in DAOPHOT. Since the number density of stars does not vary much in the field of the cluster, the add star experiment was performed on one region of the cluster for which exposure times in various filters are longer. We have added about 10% to 15% stars to each frame, and these were recovered along with the observed stars. The photometric errors are estimated from the added stars and these values for magnitudes in various filters are tabulated in Table 3. The photometric errors are a function of crowding of stars and exposure time (e.g., Sagar, Richtler, & de Boer 1991). As these two are very similar for all five clusters studied here, these photometric errors can be considered typical for the rest of the four clusters also. This method also helps to estimate the incompleteness of stars with respect to magnitude. The method for determining the completeness of the photometric data on the CCD frames using DAOPHOT has been discussed by several authors (e.g., Stetson 1987; Mateo 1988; Sagar & Richtler 1991; Sagar & Griffiths 1998

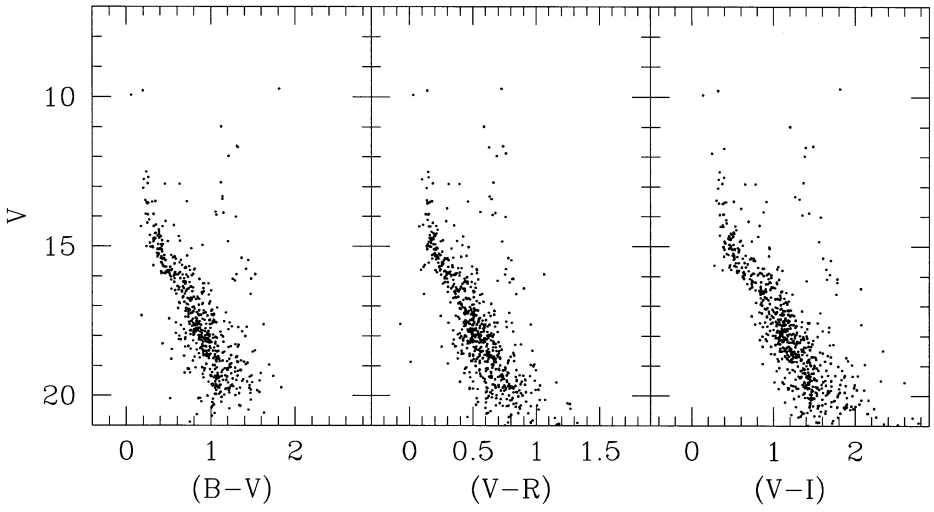

FIG. 8.—Cluster CMDs of NGC 2383 with all the stars observed are shown in the V vs. $B-V$, V vs. $V-R$, and V vs. $V-I$ planes

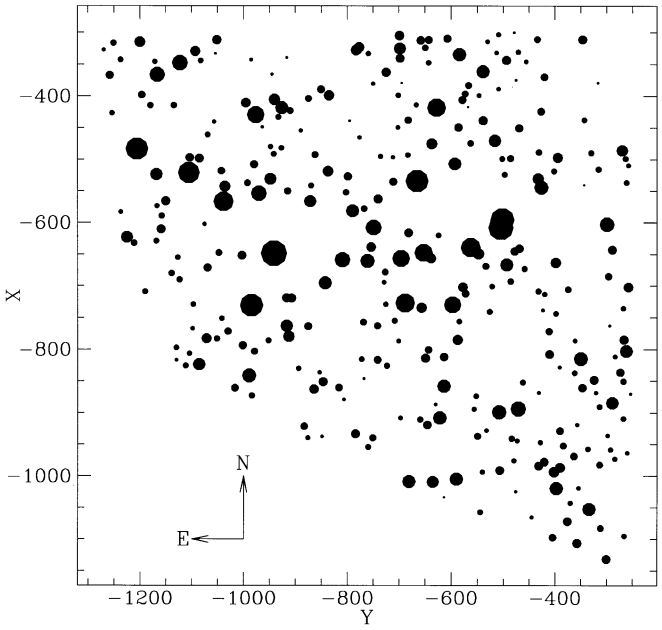

FIG. 9.—Stars observed in the cluster region of NGC 2384 are shown here.

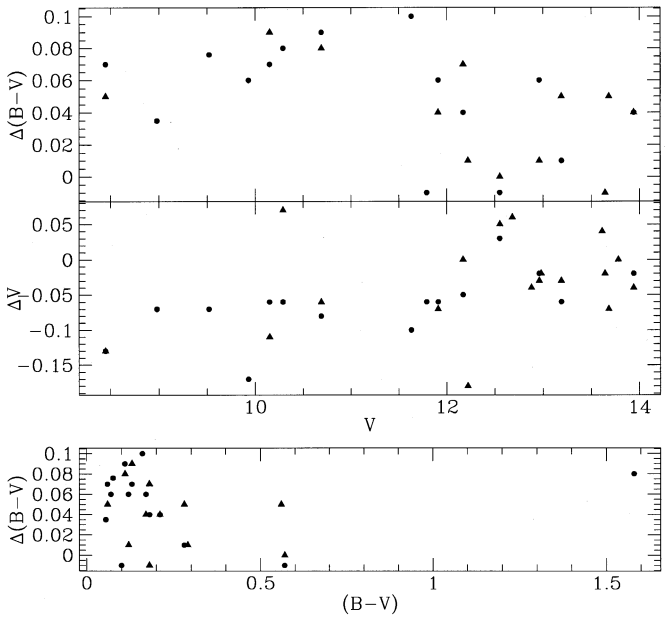

FIG. 10.—Present photometry for NGC 2384 is compared with those of Vogt & Moffat (1972) (*filled circles*) and Hassan (1984) (*triangles*). The difference is calculated such that Δ = present—earlier photometry.

and references therein). From this method, we found that the data are 100% complete up to 16.0 mag, ~95% complete up to 17.0 mag, and 80% complete up to 17.5 mag in all the filters.

5. SPECTROSCOPY AND SPECTRAL CLASSIFICATION

We have obtained the spectra for the brighter members in the cluster with the intention of identifying probable non-members. This will also help in the identification of actual evolutionary state of the stars lying on the tip of the MS. The flux calibrated spectra of the stars observed were classified with the help of the digital spectral library from Jacoby et al. (1984). This library contains spectra of 161 stars between the spectral classes O to M covering the luminosity classes V, III, and I. The spectra extend from 3510 to 7427 Å at a resolution of ~4.5 Å and sampled at 1.4 Å interval. These spectra are of individual stars and are corrected for interstellar reddening. As the library spectra is in digital form, it can be plotted over the observed spectra for a good comparison. The library spectra were normalized to 100 at 5450 Å; therefore, the observed spectra are also normalized in the same way for comparison.

TABLE 3

PHOTOMETRIC ERRORS OBTAINED FOR NGC 1912

Magnitude Range	σ_B	σ_V	σ_R	σ_I
≤15.0	0.013	0.015	0.010	0.015
15.0–16.0	0.022	0.027	0.013	0.029
16.0–17.0	0.025	0.036	0.051	0.063
17.0–18.0	0.070	0.095	0.063	0.11
18.0–18.5	0.10	0.24	0.14	0.28

NGC 1912.—We have obtained spectra for 15 stars in the cluster. The present spectral classification is tabulated in Table 4. The table also contains identification numbers, V and $B-V$ magnitudes of these stars, available membership,

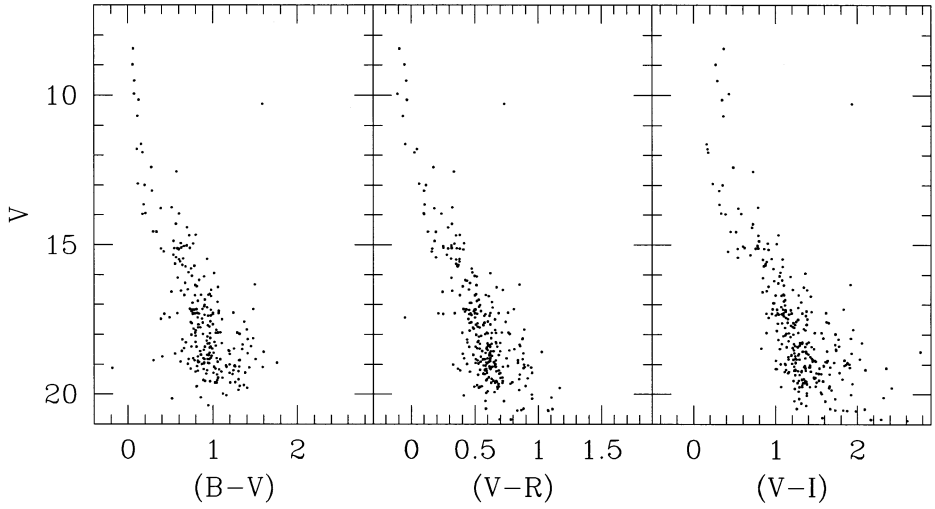

FIG. 11.—V vs. $B-V$, V vs. $V-R$, and V vs. $V-I$ CMDs are shown here for NGC 2384

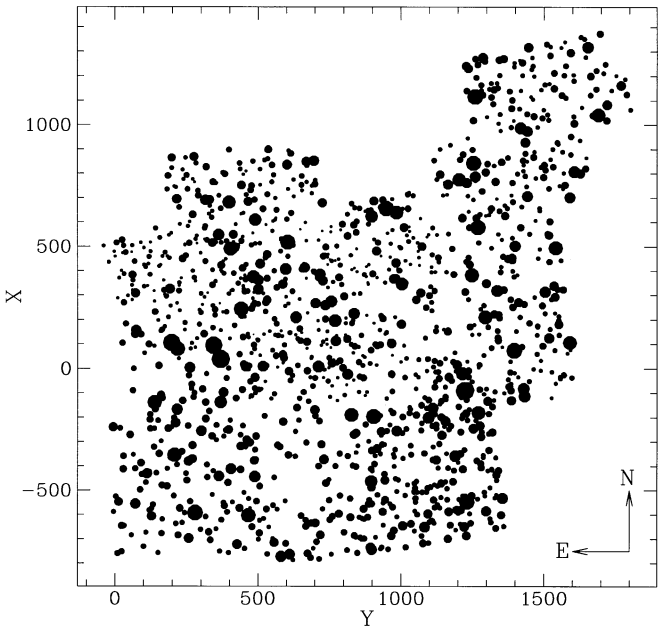

FIG. 12.—Cluster stars for which photometry is done are shown for the cluster NGC 6709.

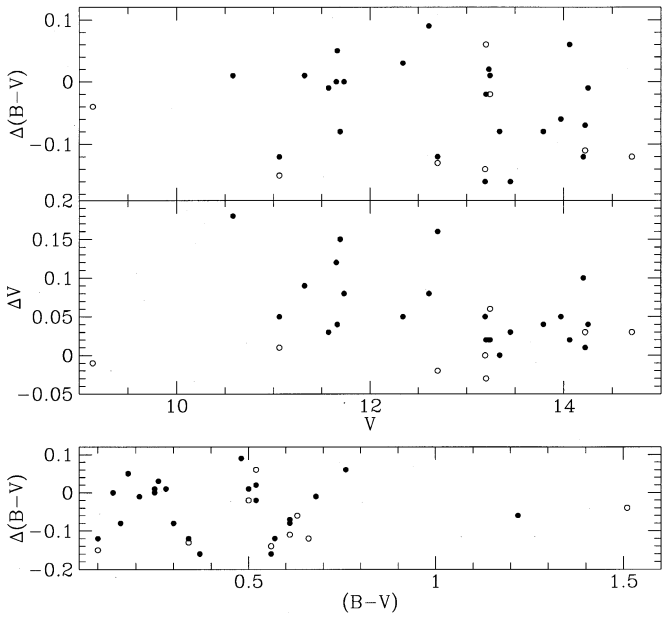

FIG. 13.—Common stars observed in NGC 6709 by Hoag et al. (1961) are compared with the present photometry. The values on the abscissa are the present value, and the difference is Δ = present—literature.

and spectral information. It can be seen that we determined comparatively late spectral types and luminosity classes compared to the determination of Hoag & Applequist (1965) for the stars S1 and S2. Hoag & Applequist (1965) used Hγ photoelectric photometry to determine the spectral types. The figure presented in their paper giving the dependence of Hγ on spectral type shows that the variation in Hγ strength across spectral type A is very small and that the turnover of the Hγ strength occurs in this spectral type. Therefore, Hγ strength is not a good parameter to determine the spectral type near A. This may be the reason for the different results obtained here. In the case of the luminosity class, it is very difficult to differentiate between an A type MS and an A type giant when we are looking at the relative flux. The positions of the stars S1 and S2 in the CMD show that their identification as giants might be correct. Considering the results from the proper motion probability given in column (7), the first seven stars in Table 4 are members. It is tempting to consider the stars S9, S29, and S3 as members based on their values of $(V - M_V)$. S9 has been found to be a foreground subgiant by Sears & Sowell (1997). Star S13 has a high value of $(V - M_V)$ and probably a nonmember as also suggested by the proper motion data. The star S28 is also known as HD 35878, and its radial velocity has been determined as −1.0, which is close to the mean value of the radial velocity for the cluster. Our spectral classification found that this has to be a foreground star; therefore we do not consider it as a member.

NGC 2383.—We have obtained spectra for six stars in this cluster. The results of the spectral classification are tabulated in Table 5. Radial velocity is not available in the literature for any of the stars. The stars S1, S2, and S8 have been observed twice and in both sets of observation the same spectral and luminosity class were obtained, as shown in Table 6. The star 2 is designated as 58440 in the HD catalog. The star S10 shows Hα in emission and shell

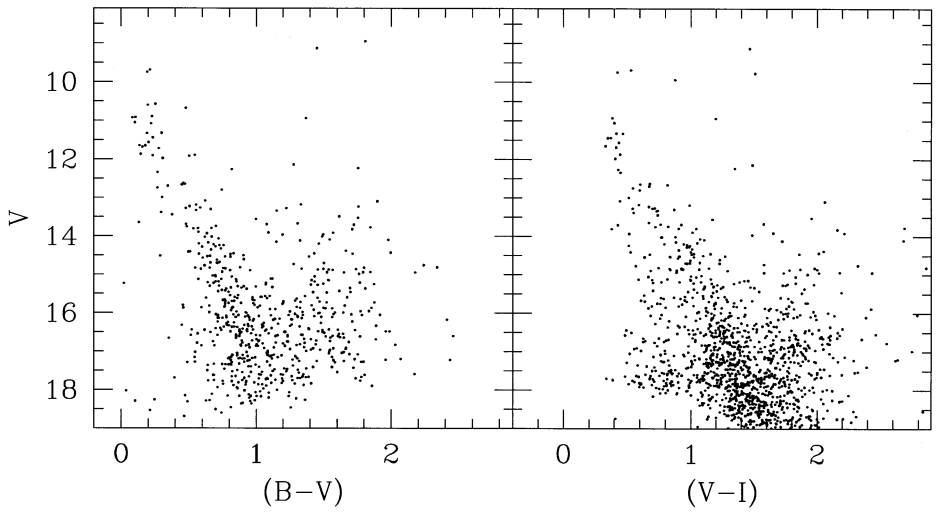

FIG. 14.—Final V vs. $B-V$ and V vs. $V-I$ CMDs of NGC 6709 are shown here

TABLE 4

RESULTS OF SPECTRAL CLASSIFICATION FOR 15 STARS IN NGC 1912

Star (1)	ID Number (2)	Spectral Classification (3)	Literature (4)	V (5)	$B-V$ (6)	Probability (7)
S20.....	11	A5 V	...	10.54	0.25	0.61
S15.....	157	A8 III	...			0.61
S5	3	G2 III	...	9.71	1.19	0.74
S23.....	29	A3 III	...			0.42
S1	49	A6 III	A2 V[1]			0.53
S2	50	A6 III	A0 V[1]			0.47
S14.....	160	A5 III	...			0.57
S9	16	F8 III	G5 IV[2]	10.27	0.65	0.0
S29.....	69	F5 III	...	10.77	0.50	0.03
S13.....	164	A6 III	...			0.0
S3	31	A8 III	...			0.25
S28.....	70	K2 I	G8 III[3]	10.18	1.21	0.24
S30.....	194	K2 I	...			0.0
S16.....	292	G9 III	...			0.0
S17.....	...	K4 III	...			...

NOTES.—Col. (1) gives the present identification number, and col. (2) gives the corresponding number in Mermilliod 1994. Present results are in col. (3), and the spectral information from the literature are in col. (4), where the superscript "1" refers to Hoag & Applequist 1965, "2" refers to Sears & Sowell 1997, and "3" refers to Sowell 1987. Cols. (5) and (6) lists the V and $B-V$ mag. The membership probability from Mills 1967 is shown in col. (7).

feature in Hβ. The shell nature cannot be confirmed as we have only one good spectra, where the shell feature is seen, but we obtained two poor spectra (due to bad sky) that showed Hα in emission. As the stars S1 and S8 are classified as supergiants, they are very bright background stars. The star S2 has a very low value of $(V - M_V)$, indicating that it is a foreground star, and those of S7, S9, and S10 are very close to each other and can be considered as members.

NGC 2384.—The results of the spectral classification are tabulated in Table 6. The star numbers referred here are that of Vogt & Moffat (1972). The classification of S11 as B3 V is very similar to the classification in the literature. The stars S1 and S10 are identified as HD 58465 and HD 58509, respectively. From the radial velocity measurements (Liu, Janes, & Bania 1989), the star 10 is suspected to be a spectroscopic binary from its variable radial velocity. Hron et al.

TABLE 5

SPECTRAL CLASSIFICATION RESULTS FOR NGC 2383

Star	ID Number	Spectral Classification	Literature	V	$B-V$
S1	1	A3 I*	B0 III[1]	9.94	0.07
S2	2	A6 III*	A3 V[1] A9 V[2]	9.80	0.24
S7	7	K3 III	...	11.69	1.27
S8	8	M1 I*	K3 III[1]	9.73	1.80
S9	9	K2 III	...	12.00	1.18
S10.....	10	A3 V(s)	...	12.76	0.22

NOTES.—The star number given in the second column corresponds to that of Vogt & Moffat 1972. The third column contains the results of the present study, the asterisk (*) refers to stars with two observed spectra, and "s" refers to shell feature. The fourth column contains the classification available already, where the superscript "1" refers to Fitzgerald et al. 1979 and "2" refers to Michigan Catalog of HD stars. The fifth and the sixth columns list the V and $B-V$ magnitudes from the present photometry.

TABLE 6

RESULTS OF SPECTRAL CLASSIFICATION FOR NGC 2384

Star (1)	ID Number (2)	Spectral Classification (3)	Literature (4)	V (5)	$B-V$ (6)
S11.....	11	B1.5 V B3[2]	B3 IV[1]	9.96	0.07
S12.....	12	B3 V	B8[2]	11.63	0.16
S13.....	13	B1.5 V	B8[2]	10.70	0.11
S14.....	14	K4 III	A5[2]	10.29	1.58

NOTES.—The star numbers in col. (2) are as in Vogt & Moffat 1972. The present results are shown in col. (3). The spectral information from the literature is given in col. (4), where the superscript "1" refers to Fitzgerald et al. 1979, and "2" refers to Babu 1985. The cols. (5) and (6) list the V and $B-V$ magnitudes from the present photometry.

(1985) find that stars 1, 2, and 10 have variable radial velocities. The star S11 has four determinations (Hron et al. 1985; Liu et al. 1989, 1991), and three of them give almost the same value, with mean value as 57.5 km s^{-1}. The average values of radial velocity for 1, 2, 8, 10, and S11 are similar, indicating that these may be cluster members. The spectral classification of S11 and S12 shows that they are MS stars and can be members. The star S14 has to be a foreground star with smaller reddening, $(V - M_V)$ and radial velocity, as found by Vogt & Moffat (1972).

NGC 6709.—We have obtained spectra for 12 stars in the cluster, and results in the tabular form can be seen in Table 7. This contains the identification number as in Mermilliod (1994), HD number if available, and the spectral information available in the literature.

When we compare the spectral class as given in Table 7, it is seen that the present determination estimates comparatively late spectral types as well as luminosity classes when compared with the estimations available. Hoag & Applequist (1965) have classified using Hγ values, which may not be a good indicator as explained earlier. Moreover, the present analysis uses a standard library with a good coverage of all spectral types and luminosity classes. This may explain the discrepancies with respect to the other results. The radial velocity values given in Table 7 are the average of the values available from Hayford (1932), E. Glushkova (1993, private communication), and Sowell (1987). The letter "v" denotes that the values obtained in various estimations are different and hence that the radial velocity may be variable. The stars S2a and S2b lie close to each other and were noted as visual doubles by Jeffers, van den Bos, & Greeby (1963). Schild & Romanishin (1976), in their study of Be stars in clusters, found stars S5 and S2a to be candidates. We do see Hα emission for S2a, but no Hα emission is seen for the star S5. Either the star has a varying emission such that this particular spectra does not show any emission or the star has ceased to have Hα emission. The second reason is possible as the present spectrum was taken after a span of about 30 yr, and this duration is long enough for the emission to disappear in Be stars. The spectra of the star S2a obtained by Sowell (1987) shows that it is a shell star. We obtained three spectra of this star on different nights. At the present resolution, no shell feature was observed, though the Hα emission is present in all the spectra. Also, we classify the spectra as that of A6 giant. This is consistent with its location on the cluster CMD. This star has a 12μ flux of 0.379 Jy, which corresponds to an IR excess of 0.316 (Sowell 1987). The membership probability information from Hakkila et al. (1983) shows that only four of the observed stars S201, S10, S11, and S2a are members of the cluster. Sears & Sowell (1997) had four common stars, of which they found S2b to be a putative member apparently ascending the RGB.

6. DESCRIPTION OF THE OBSERVED COLOR-MAGNITUDE DIAGRAMS

In order to identify the various sequences in the CMD, we have demarcated the region with only field stars and the region with the evolved stars in the V versus $B-V$ CMDs as shown in Figures 15 and 16. To the left of the slanting line lies the cluster MS. Here, the cluster MS stars along with the field stars are present. The right side of the slanting line contains only the field stars. The stars lying above the horizontal line are the candidates for cluster red giants.

The evolutionary features as seen in individual clusters are discussed below.

NGC 1907.—The stars observed in the cluster region of NGC 1907 are shown in the V versus $B-V$ CMD in the Figure 15. The stars that are not observed, but present in Hoag et al. (1961), are included in this figure. There seems to be a lot of spread in the cluster MS, suggesting large amount of differential reddening. The Lyngå catalog also notes this by the letter "v" next to the reddening value of 0.42. NGC 1907 has a wide and well-populated MS extending up to 12 mag in the brighter end and up to 18 mag in V in the fainter end. The turn-off color in $B-V$ is $\sim$0.5 mag. The three stars that are more than 1.5 mag brighter than the turn-off might be field stars. The stars falling to the left of the MS can be assumed to be foreground stars. The scatter seen near the turn-off may be due to the presence of differential reddening apart from that due to binaries. A clump of stars seen near $V = 12.5$ mag and $(B-V) = 1.4$ mag are the red giants. Though the red giant clump is seen, the red giant branch is not visible. The stars that lie below this clump and

TABLE 7

SPECTRAL CLASSIFICATION FOR THE OBSERVED SPECTRA IN NGC 6709

Star (1)	ID Number (2)	HD Number (3)	Spectral Classification (4)	Literature (5)	V (6)	$B-V$ (7)	Probability (8)	V_r (9)
S1a,b.....	...		A6 III	...	...			
S2b.....	208		K4 III	K2 Ib(1), K2 II(2)	9.13	1.45	0.06	−11.2
S3	303	229716	K3 III	G8 III/IV(1), G8 III(2)	8.95	1.81	0.20	−14.0v
S5	293		A6 III	A0 V(3), B9 V(4), A0 V(2)	10.92	0.11	0.40	
S7	...		A6 V	...			0.0	
S6	291		A6 V	...	10.58	0.25	0.0	
S201	201		A6 III	B9 V(4)	10.60	0.20	0.65	
S10.....	372	229700	A5 III	A0 V(3)/A0 II–III(4)			0.85	−21.0v
S11.....	337	229715	A6 III	B9 V(4), B8 V(2)	10.68	0.48	0.79	
S44.....	413	229684	A3 V	B6 III(4)			0.0	+22.0
S2a.....	209	174715	A6 III(Hα em)	...	9.70	0.21	0.84	
S17.....	277		A3 III	...	10.93	0.08	0.0	

NOTES.—The second column refers to the identification number in Mermilliod 1994. Some stars are in the HD catalog; their numbers are given in col. (3). The present classification is given in col. (4). The spectral information from the literature for stars available are shown in the col. (5). The references are given in the parenthesis, where "1" refers to Sowell 1987, "2" refers to Sears & Sowell 1997, "3" refers to Young & Martin 1973, and "4" refers to Hoag & Applequist 1965. The V and $B-V$ mag of the stars from the present photometry are listed in cols. (6) and (7). The membership probability from Hakkila et al. 1983 is shown in col. (8). The mean radial velocity is shown in the last column.

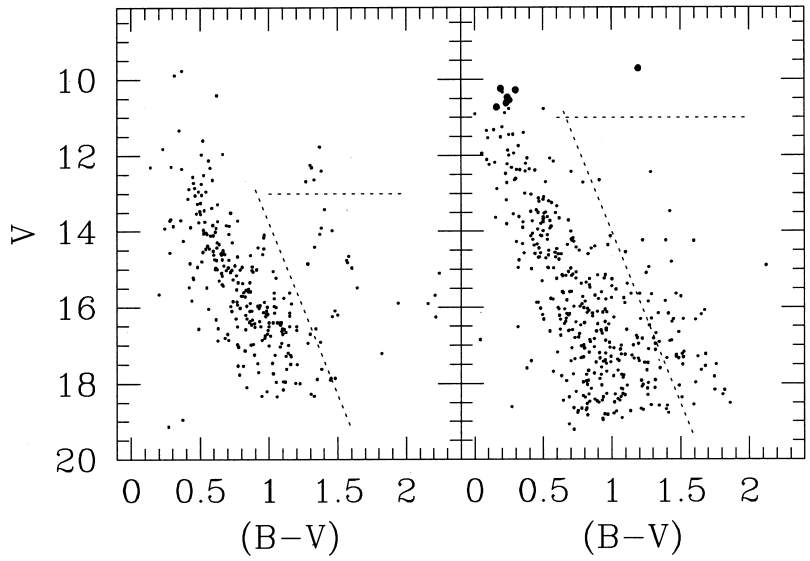

FIG. 15.—CMDs of two open clusters (*left*, NGC 1907; *right*, NGC 1912) are shown here with the different regions identified. The stars for which the spectra are obtained are shown as bigger dots.

to the right of the MS are assumed to be field stars as the cluster is not young enough to have pre-MS stars in this region.

NGC 1912.—We used the proper motion probability from Mills (1967) to identify the members from our data and also from the photoelectric and photographic data of Hoag et al. (1961). A histogram plot of the probability versus the number of stars using the data in Mills (1967) as shown in Figure 17 tells us that there is a clear demarcation between the cluster members and the field stars and that the cluster population has a membership probability greater than 0.40. Hence, we have considered stars with probability values less than 0.40 as nonmembers, and these stars are not considered in the further analysis of the cluster. The final V versus $B-V$ CMD consists of the present data excluding the nonmembers and the member stars from Hoag et al. (1961), which were not observed by us. This is shown in Figure 15.

The cluster NGC 1912 has a very wide MS, which is more than what the variable reddening found in that region can account for. The MS extends up to 10 mag in V in the brighter end and up to 19 mag at the fainter end, which is the limiting magnitude in V. The data can be assumed to be complete up to 16 mag in V, as the photographic data are also included. Up to 15 mag in V, the probable nonmembers have been removed using the proper motion data of Mills (1967), and only the remaining stars are shown in the figure. In this magnitude range, the stars are seen to be distributed in a clumpy fashion along the MS giving rise to gaps in between, which is also observed in the V versus $V-I$ CMD. There is a large clump of stars lying 0.2 mag to the right of the MS near $V = 13.5$ mag. Most of the stars in these clumps are proper motion members, which means that their presence needs to be accounted for. The above-mentioned features as well as the presence of stars on the right of the MS indicate that most of the stars might be peculiar like fast rotators, binaries, or stars with spots. There is only one star seen as a red giant candidate. Though the star is a probable member, it seems to be too blue to be a red giant.

NGC 2383.—The observed stars are shown in the V versus $B-V$ CMD presented in Figure 16. The cluster

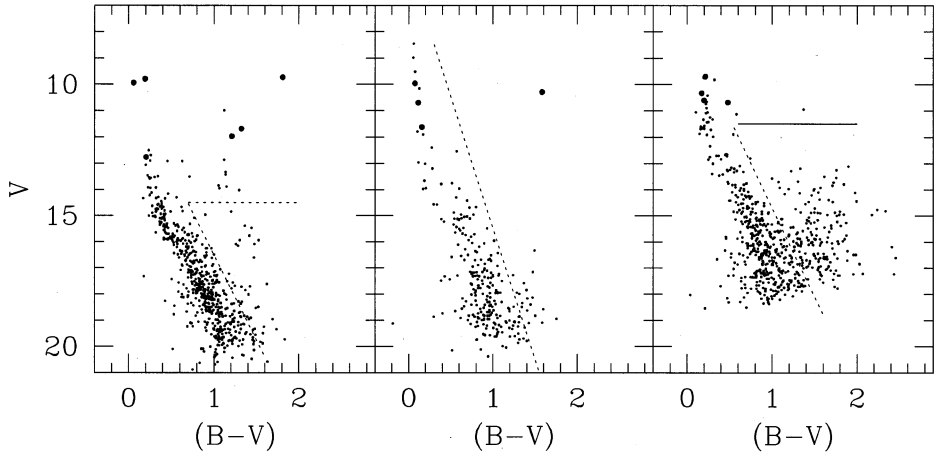

FIG. 16.—CMDs of three open clusters (*left*, NGC 2383; *middle*, NGC 2384; *right*, NGC 6709) are shown here with the different regions identified. The stars for which the spectra are obtained are shown as bigger dots.

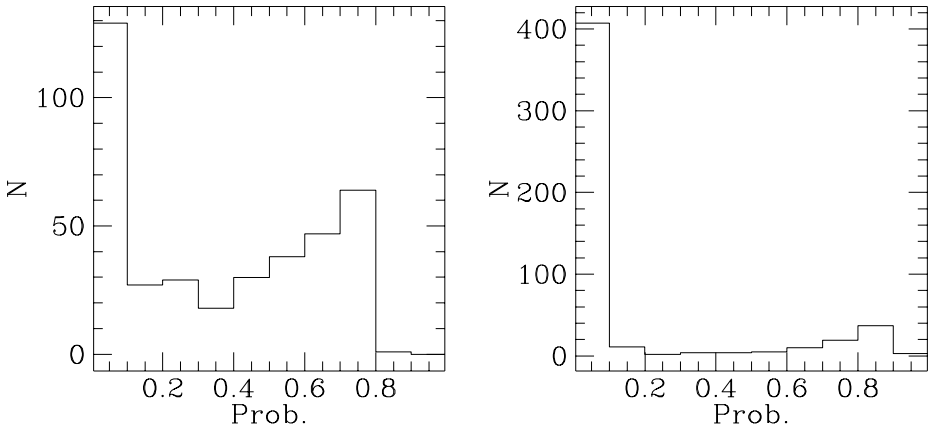

FIG. 17.—Membership probability distribution for the clusters NGC 1912 (*left*) and NGC 6709 (*right*). We have used Mills (1976) data for NGC 1912 and Hakkila et al. (1983) for NGC 6709.

NGC 2383 has a well-defined MS as seen in all three CMDs. The MS turn-off is near $V \sim 12.7$, $(B-V) \sim 0.2$, $V-R \sim 0.1$, and $V-I \sim 0.3$ mag. The stars were seen populated continuously up to 14 mag in the MS, and above this only a few stars were seen up to the turn-off. The scatter in the MS is less, which might indicate the absence of significant number of binary stars. The two bright stars around $V = 10$ mag are nonmembers. The subgiant branch is seen more clearly in the V versus $V-R$ CMD (see Fig. 8). A few stars are seen scattered near the location for the red giant clump. The isochrone fitting, as discussed later, showed that the clump consists of the brighter three of these seven stars at $V = 14$ mag and $(B-V) = 1.1$ mag. Three stars are also seen just above the clump (big dots), of which the brightest star at $V = 9.7$ mag and $(B-V) = 1.8$ mag is estimated to be a background star from spectra, and the other two may be members.

NGC 2384.—The cluster CMD in V versus $B-V$ is shown in Figure 16. The cluster NGC 2384 seems to be very young compared to other clusters. The MS is extending up to ~ 8.5 mag in V at the brighter end. There seems to be a gap in the MS below 15 mag in V, which is more clearly seen in the V versus $V-R$ and V versus $V-I$ CMDs (see Fig. 11). The stars lying to the right of the MS at this V magnitude may be pre-MS stars. In that case, the stars lying fainter than 16 mag should mainly be field stars. The single star at $V \sim 10$ mag and $B-V \sim 1.6$ mag cannot be a cluster member as seen from the spectral classification. There are no other evolved stars seen in the CMD. The width of the fainter MS is very low, indicating that the percentage of binary stars present could be very low.

NGC 6709.—We include the stars that are not observed here, but for which photoelectric or photographic measurements are available. The proper motion information available from Hakkila et. al. (1983) showed that there is a strong field population near the proper motion probability 0.0 and that the cluster members generally lie above the probability of 0.60 (see Fig. 17). Thus, we consider stars with probability greater than 0.60 as members. The stars thus identified as members from photoelectric and photographic data are plotted together with the present data in the V versus $B-V$ CMD as shown in Figure 16. The stars identified as members in the present data are shown by different symbols in the figure and the nonmembers are excluded. The cluster NGC 6709 has a CMD mostly embedded in the field stars. This is evident from the proper motion data of Hakkila et al. (1983). The turn-off is around 9.5 mag in V, 0.2 mag in $B-V$, and 0.3 mag in $V-I$. The photographic data are included up to 15.5 mag in V and the photoelectric data in the bright end. All the nonmembers up to 16 mag in V have been removed using the proper motion data, and only the remaining stars are shown in the figure. The MS is well populated between 10.5 and 12.0 mag in V in the bright end and three stars are seen above this at 9.5 mag. There seems to be a gap between 12.0 and 12.7, where only one star is present. There is again a gap between 13.0 and 13.5 mag in V. After $V \sim 14$ the MS is continuous. The gaps mentioned above can also be seen in the V versus $V-I$ CMD. The clumpiness of stars in the MS is similar to that seen in the CMD of NGC 1912. There is only one candidate red giant star. As the data can be considered to be complete toward the brighter end, the cluster actually has only one red giant.

6.1. *Gap in the MS*

A gap in the MS is loosely defined as a band, not necessarily perpendicular to the MS, with no or very few stars. Böhm-Vitense & Canterna (1974) first located a gap on the MS around $(B-V)_0 = 0.27$ mag, due to the onset of convection in the envelope. The gaps found in open clusters were listed by Kjeldsen & Frandsen (1991), and some of the gaps have physical explanations. Phelps & Janes (1993) and Wilner & Lada (1991) also discussed gaps in open clusters.

In three of the five clusters, gaps at various points in the MS of the CMDs are noticed. The details of the gaps found in the three cluster CMDs are given in Table 8. The probability for these gaps to be accidental was estimated using the method adopted by Hawarden (1971), and the probability values obtained are also tabulated. All the gaps listed in the table have very low probability to be accidental, and hence they are expected to be real gaps. The cluster MS of NGC 1912 is seen to be clumpy with many gaps, and the prominent one is listed in the Table 8, which lies a little below the MS turn-off. Another feature seen in this cluster MS is that, the stars near $M_V \sim 1.5$ seems to be shifted to redder $B-V$ resulting in a gap in the MS and a clump of stars to the right of this, which are similar to the A-bend and A3-group found by Kjeldsen & Frandsen (1991). Two gaps are noticed in NGC 2383, of which the first one may be the Mermilliod gap (Mermilliod 1976), but the $(B-V)_0$ values differ by 0.1 mag. The first gap seen in the case of

TABLE 8

DETAILS OF THE GAPS NOTICED IN THE MS OF THE THREE CLUSTER CMDS

CLUSTER	M_V	$(B-V)_0$	WIDTH IN M_V	WIDTH IN $(B-V)_0$	PROBABILITY
NGC 1912.....	−0.9	0.0	0.1	0.1	0.09
NGC 2383.....	−0.1	0.0	0.15	0.05	0.12
	0.35	0.05	0.05	0.05	0.08
NGC 6709.....	1.15	0.00	0.15	0.05	0.02
	1.5	0.1	0.1	0.1	0.04

NGC 6709 is similar to the A-group, and the second one is similar to the M11-gap (Kjeldsen & Frandsen 1991). The gap found in NGC 1912 and the second gap in NGC 2383 are not similar to any of the gaps mentioned in Kjeldsen & Frandsen (1991).

7. REDDENING AND DISTANCE

The method used to determine reddening and distance from the present photometric data is by the fitting of ZAMS to the MS of the cluster CMD. We have the cluster CMDs in V versus $B-V$ and V versus $V-I$ and, in some cases, V versus $V-R$ also. The simultaneous fitting of same apparent distance modulus, $(V-M_V)$ to all the CMDs give the values of reddening $E(B-V)$, $E(V-R)$, and $E(V-I)$.

We also used another method to determine the reddening $E(B-V)$, from the color-color plot of $(B-I)$ versus $(B-V)$. The method was discussed in Natali et al. (1994) and presented a parameter that can be used to determine the interstellar reddening. The relation between $(B-V)$ and $(B-I)$ is given as

$$(B-I) = \beta(B-V) + E(B-V)(2.64 - \beta) .$$

Therefore,

$$E(B-V) = \frac{C}{(2.64 - \beta)} ,$$

where C is the y-intercept and β is the slope.

Once the reddening is estimated, the extinction in the V magnitude can be determined using the relation $A_V = R \times E(B-V)$. The value of R is assumed to be 3.1. The intrinsic V magnitude then becomes $V_0 = V - A_V$. The distances to the clusters are found from the estimates of absolute distance modulus $(V_0 - M_V)$. The absolute distance modulus is related to distance by the relation, $(V_0 - M_V) = 5 \log D - 5$. From this relation, the distance to the cluster D in parsecs can be computed.

7.1. *Estimation of Errors*

The uncertainties associated with the reddening and distance determinations using the methods described above are discussed below.

Reddening.—The errors in the determination of reddening mainly arise from the uncertainties in intrinsic colors of the stars that constitute the unreddened MS. The reddening estimated using the first method is by visual fitting of ZAMS to the cluster MS and the uncertainty in the visual estimate is ∼0.02 mag. Therefore, the uncertainty in $E(B-V)$ is

$$\sigma^2_{E(B-V)} \sim 0.02^2 + \sigma^2_{(B-V)_0} .$$

Schmidt-Kaler (1982) estimated that $\sigma_{(B-V)_0} \sim 0.04$ mag Thus, the uncertainty in $E(B-V)$ is $\sigma_{E(B-V)} \sim 0.05$ mag.

The second method uses the relation

$$E(B-V) = \frac{C}{(2.64 - \beta)} .$$

The uncertainty in $E(B-V)$ is

$$\sigma^2_{E(B-V)} \sim \sigma^2_C + \sigma^2_\beta .$$

The values of σ_C and σ_β are evaluated in individual cases.

Distance.—The distance is estimated using the fitting of ZAMS to the cluster MS. A detailed analysis of the uncertainty in the distance estimate was done by Phelps & Janes (1994). They estimated that the uncertainty in the determination of absolute distance modulus, $\sigma_{(V_0-M_V)}$ is mainly dominated by the error in the calibration of M_V, which is $\sigma_{M_V} \sim 0.3$ mag, and the total uncertainty in the absolute distance modulus is $\sigma_{(V_0-M_V)} \sim 0.32$ mag. This gives rise the uncertainty in the distance,

$$\sigma^2_D = 0.213 D^2 \sigma^2_{(V_0-M_V)} ,$$

where D is in parsecs. The uncertainty in the relative distances is much less if the fitting of ZAMS are used for all the clusters in the sample. In this case, the systematic error in absolute distance modulus reduces to $\sigma_{(V_0-M_V)} \sim 0.10$ mag. As the uncertainty in distance is a function of distance, the errors are determined when the individual cluster distances are estimated.

Fitting of the ZAMS was done to the individual clusters, and the results are tabulated in Table 9. The CMDs of clusters fitted with ZAMS are also shown in Figures 18, 19, 20, 21, and 22 for NGC 1907, NGC 1912, NGC 2383, NGC 2384, and NGC 6709, respectively. The star S10 (HD 229700; HIP 92486) in NGC 6709 has been observed by *Hipparcos* and the parallax for this star is measured as1.00 ± 1.70 mas. Therefore, the mean distance to this star is 1000 pc, which is very close to the value obtained by us (1190 ± 175 pc).

The reddening results using both the methods are also tabulated in Table 9. To obtain reddening using the second method, we plotted $(B-I)$ versus $(B-V)$ as shown in Figure 23 and fitted a straight line using a least squares fit, iteratively removing the stars that are lying off by more than 3 σ from the straight line. In all the cases, the correlation coefficient of the least-squares fit is ∼0.98.

The $E(B-V)$ estimate using the two methods seems to agree well in the case of three clusters. In the case of NGC 6709, the ZAMS fitting estimates 0.20 ± 0.05, whereas the second method estimates 0.35 ± 0.03 mag for $E(B-V)$. The second method uses all the stars observed in the field. It can be seen from the figure, which shows the membership prob-

TABLE 9

RESULTS OF THE DISTANCE AND REDDENING DETERMINATIONS OF THE OPEN CLUSTERS UNDER STUDY

CLUSTER	$(V - M_V) \pm 0.3$	$E(B-V)$ 1(± 0.05)	$E(B-V)$ 2	$E(V-R)$	$E(V-I)$	D (pc)
NGC 1907.....	12.5	0.40	...	...	...	1785 ± 260
NGC 1912.....	12.0	0.23	0.25 ± 0.03	...	0.33	1810 ± 265
NGC 2383.....	13.3	0.22	0.22 ± 0.02	0.10	0.35	3340 ± 490
NGC 2384.....	13.2	0.28	0.22 ± 0.03	0.05	0.40	2925 ± 430
NGC 6709.....	11.0	0.20	0.35 ± 0.03	...	0.37	1190 ± 175

ability distribution in the region of this cluster, that this region is dominated by the field stars. Hence, it is possible that this method determines the reddening of the Galactic field near NGC 6709, rather than the reddening toward the cluster.

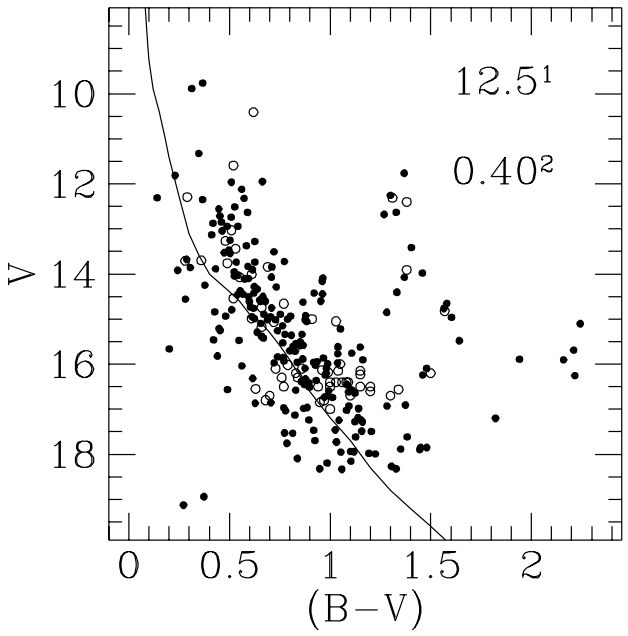

FIG. 18.—Cluster CMD of NGC 1907 is fitted with ZAMS to obtain the reddening and distance. The estimated value of $(V-M_V)$ is indicated by the superscript "1" and reddening by "2."

8. LUMINOSITY FUNCTIONS

In order to obtain the main-sequence luminosity function (MSLF) of the cluster, elimination of the field stars from the MS is done in two ways. The first method uses the proper motion data, and the second one is a statistical method. For the clusters, NGC 1912 and NGC 6709, the field stars from the observed MS are eliminated using the proper motion data. In the case of NGC 1912, the MS up to 15 mag in V can be considered as devoid of field stars, and for NGC 6709, the MS up to 14 mag in V is considered. The data are complete up to a magnitude of 16.0 in V, as seen from the results of the artificial addstar experiment. This method of eliminating field stars cannot be used if no proper motion data are available in the field of the cluster. An alternate method is to observe a nearby region and find out the number of field stars in each magnitude bin and hence is a statistical method. Other studies (e.g., Wilner & Lada 1991; Phelps & Janes 1993) have also used the statistical approach to determine luminosity functions. The field region was observed only for the clusters NGC 2383 and NGC 2384. As the clusters lie very close to each other the same region was considered as field to both the clusters. The CMD of the observed field region is shown in Figure 24. The CMDs show that most of the field stars are fainter than 15 mag in V and that only a few stars are present brighter than this. This CMD can be used to eliminate the field star contamination in the CMDs of NGC 2383 and NGC 2384. In order to get the MSLF, the cluster stars that are in the MS and below the turn-off were binned in V magnitude. After correcting for the difference in area between the cluster and the field regions, the number of stars obtained

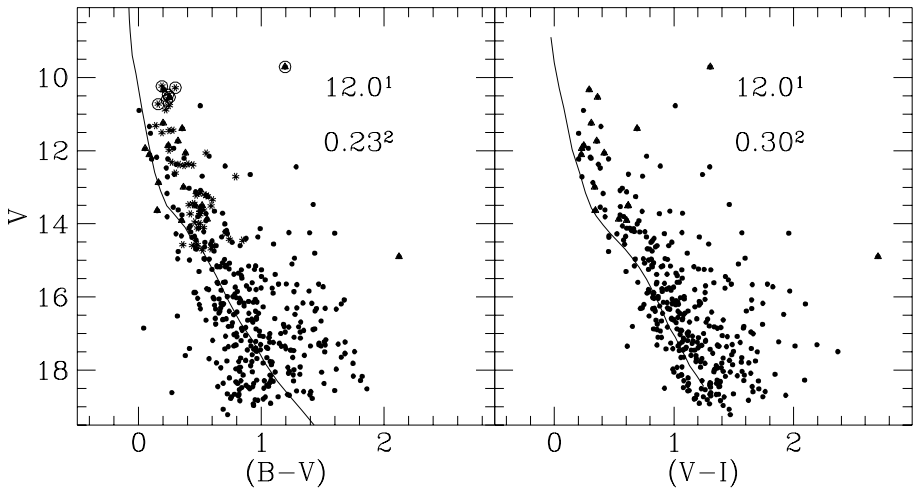

FIG. 19.—CMDs of NGC 1912 fitted with ZAMS are shown here. The values of $(V - M_V)$ are shown with superscript "1," and reddening with superscript "2."

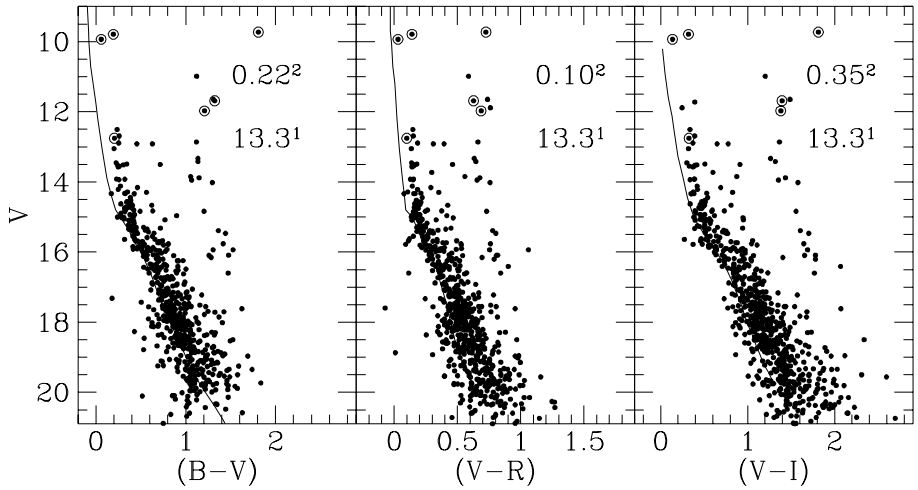

FIG. 20.—V vs. $B-V$, V vs. $V-R$ and V vs. $V-I$ CMDs of NGC 2383 are fitted with ZAMS. The values of $(V - M_V)$ are shown with superscript "1," and reddening with superscript "2."

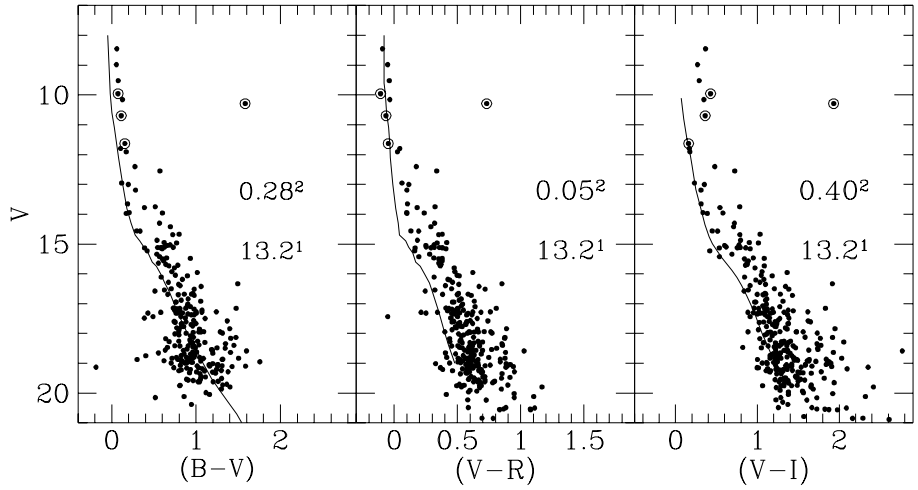

FIG. 21.—ZAMS is fitted to the cluster CMDs of NGC 2384. The superscript "1" refers to the $(V - M_V)$, and "2" refers to the reddening.

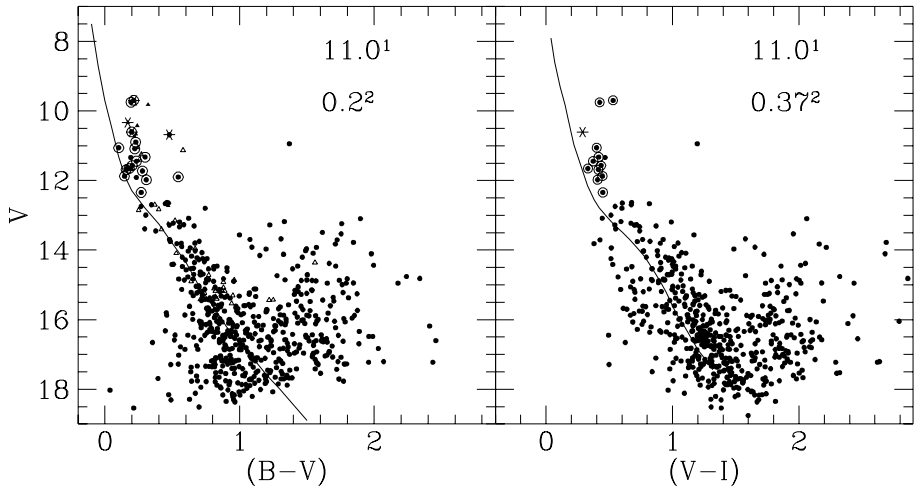

FIG. 22.—V vs. $B-V$ and V vs. $V-I$ CMDs of NGC 6709 are fitted with the ZAMS. The values of $(V - M_V)$ are shown with superscript "1," and reddening with superscript "2."

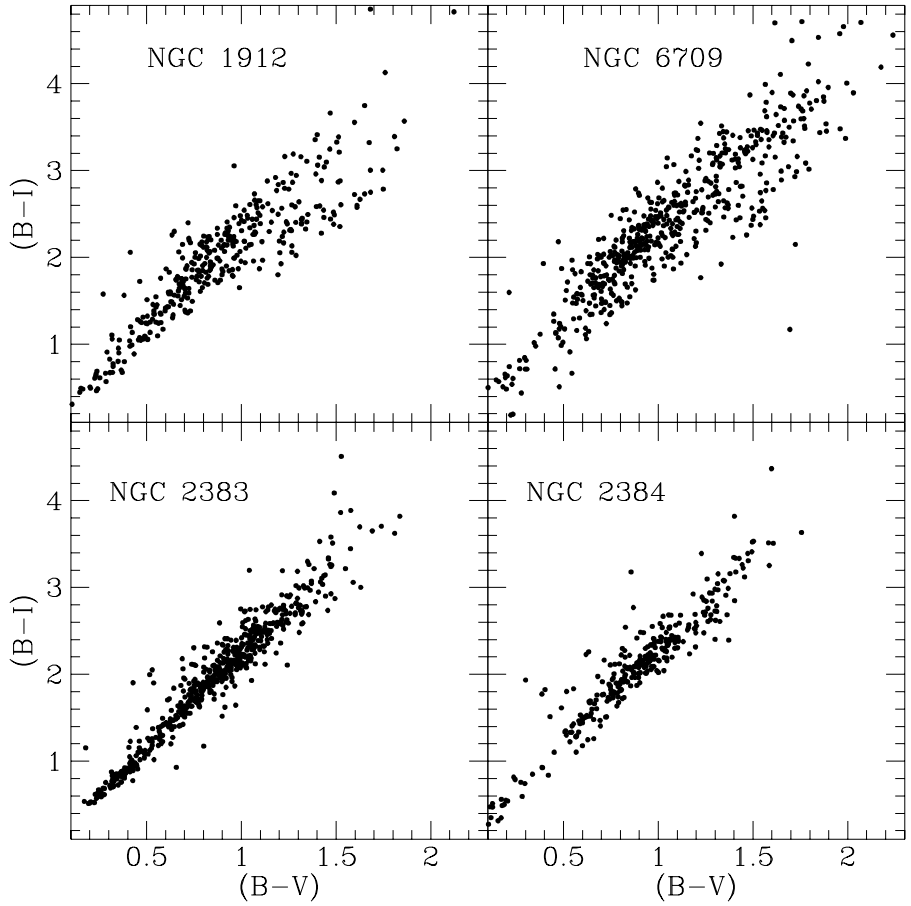

FIG. 23.—Color-color plot of $(B-I)$ vs. $B-V$ is shown here, which is used to find the reddening as explained in the text

from the field region in each magnitude bin was subtracted from the number obtained from the cluster frame, which gives the actual number of cluster stars. The MS LFs are found for four clusters. The estimate of the field star density was not determined or available for the cluster NGC 1907, and it was excluded from this analysis. The MSLF for the four clusters are shown in Figure 25. In the case of NGC 2383 and NGC 2384, the MSLF before the field star subtraction is also shown.

One expects the number of cluster stars to increase more toward the fainter magnitudes, because of the nature of the mass function. The MSLF of NGC 1912 rises steadily as expected. In the case of NGC 2383, it rises in a jumpy fashion. There seems to be lesser number of stars in these clusters fainter than 15.5 mag. This cannot be an artifact due to incompleteness, as the crowding is very low at this magnitude. The most probable reason may be that, as the cluster is a few times 10^8 yr old, it might have lost the

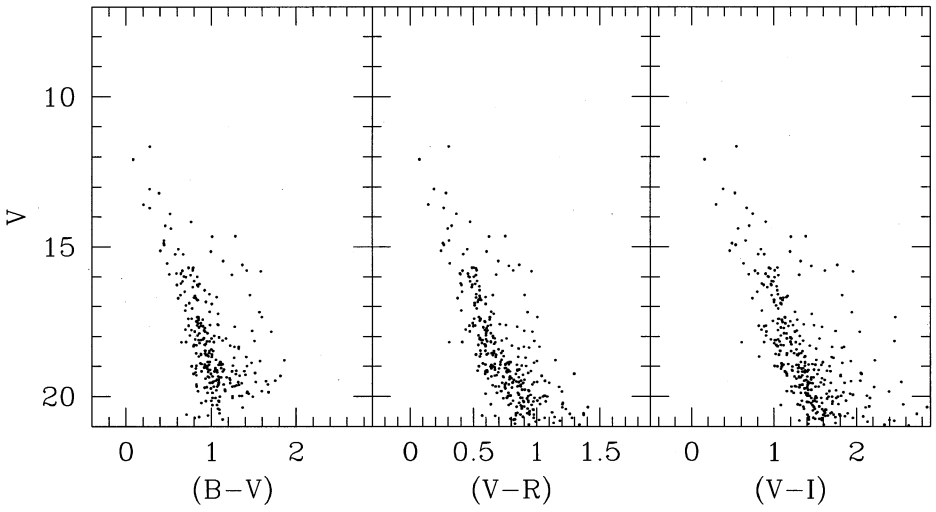

FIG. 24.—CMDs of the field region for the clusters NGC 2383 and 2384 are shown here

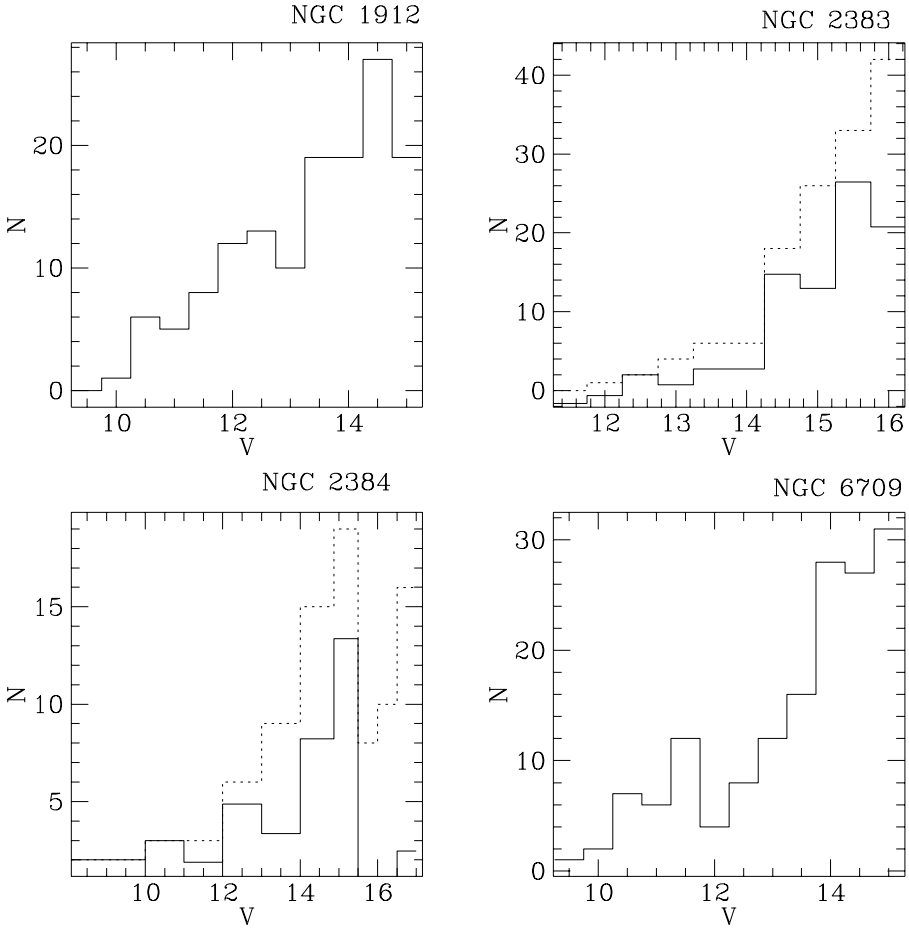

FIG. 25.—MSLF for the clusters NGC 1912, NGC 2383, NGC 2384, and NGC 6709 are plotted as solid lines. The dotted lines show the MSLF before field star subtraction.

low-mass stars due to dynamical evolution. In the case of NGC 2384, the initially rising MSLF falls after $V \sim 15$ mag. This drop of the LF might indicate that the cluster MS ends here as the cluster is quite young to relax dynamically. If the stars below this V magnitude are in the pre-MS phase, then one expects to see them to the right of the MS. As no stars are seen in the pre-MS phase also, one may conclude that the stars are not formed below the mass corresponding to this magnitude. The MSLF of NGC 6709 also shows a dip around 12 mag in V, which corresponds to the gap discussed above.

9. AGE DETERMINATION

In order to determine the age of clusters, we used three stellar evolutionary models consisting of one classical and two overshoot models. The classical model used here is by Castellani et al. (1990) and is referred to as model 1. It covers a mass range of 0.8–20 $M_\odot$. The model given by Schaller et al. (1992) is our model 2, these cover a mass range of 0.8 $M_\odot$ to 120 $M_\odot$. Bressan et al. (1993) presented evolutionary models in the mass range of 0.6 to 120 $M_\odot$ and this is our model 3. Models 2 and 3 incorporate the effects due to overshooting of the convective core. The Z value considered is 0.02 for all the models. We considered only solar metallicity as the clusters analyzed are of young/intermediate age.

The age of the clusters was determined by comparing the cluster sequence with the isochrones from the models. The isochrones corresponding to model 3 were obtained from Bertelli et al. (1994). The isochrones for models 1 and 2 were computed. The isochrones were converted from the log $L/L_\odot$ versus log $T_{\rm eff}$ plane to the M_V, $(B-V)_0$ plane using color-temperature relations and bolometric corrections from Kurucz (1979) and VandenBerg (1983) complemented with values given by Johnson (1966) for the temperatures below 4000 K. The isochrones are fitted to the cluster CMDs as shown in Figures 26, 27, 28, 29, and 30 for the clusters NGC 1907, NGC 1912, NGC 2383, NGC 2384, and NGC 6709, respectively. The ages of the clusters as found from the three models are tabulated in Table 10.

The isochrones for models 1 and 2 were constructed only in M_V versus $(B-V)_0$ plane. As the isochrones from model 3 are also available in the other two colors $(V-R)_0$ and $(V-I)_0$, these were fitted in the M_V versus $(V-I)_0$ for four clusters (except NGC 1907) and also in the M_V versus $(V-R)_0$ plane for NGC 2383 and NGC 2384. The isochrone of the same age fits the CMDs in all the planes. The turn-off region of the clusters are well reproduced by all isochrones. As seen from Table 10, except NGC 2384, the rest of the four clusters are of intermediate age. The overall morphology at the turn-off is same for the three models. The base of the red giant branch is extended more to the cooler side in the isochrones of model 3. This may be a result of using different color- temperature relations with respect to those used here. In the case of models 1 and 2, the isochrones of model 2 run redder than those of model 1. The

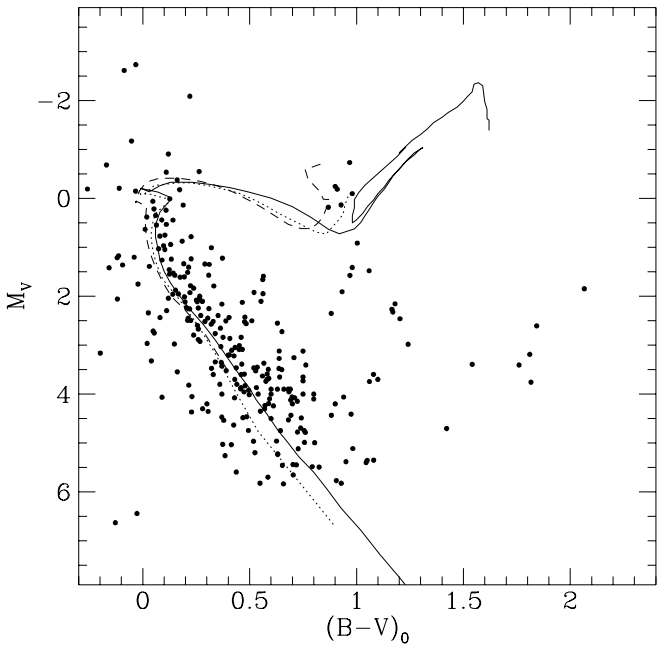

FIG. 26.—Isochrones are fitted to the cluster sequence of NGC 1907. The solid line is the one from model 3, the dotted line is from model 2, and the dashed line is from model 1.

conversion problem is not here as the same relations are used, therefore this may be due to the difference in mixing length used in the calculation of envelope convection. For clusters in which the red giant clump is seen, like NGC 1907 and NGC 2383, the isochrones need to be redder in the case of model 1. The difference between classical and overshoot models are not very clear from this comparison. One point to be noticed is that the isochrones of models 2 and 3 fit the MS well for the estimated values of reddening. In the case of model 1, the isochrones are falling bluer in $(B-V)_0$ than the cluster sequence as well as the other isochrones. We have shifted the model 1 isochrones by 0.03 mag in $(B-V)_0$ toward red to match the sequence. The classical model, model 1, found a younger age for the clusters compared to the overshoot models. In the case of the older four clusters, models 2 and 3 find the same age. For the younger cluster, NGC 2384, model 3 finds an older age compared to model 2. The present age determinations for NGC 1907 and NGC 1912 are very close to the values given in Lyngå (1987). In the case of NGC 2383, the present determination shows that the cluster is much older than the previously estimated value. Also, the clusters NGC 6709 and NGC 2384 turn out to be older than the ages given in Lyngå (1987).

10. SYNTHETIC COLOR-MAGNITUDE DIAGRAMS AND LUMINOSITY FUNCTIONS

The idea is to generate a CMD having the same age and chemical composition as the observed cluster CMDs, with the help of the theoretical stellar evolutionary tracks of various masses. The computer code developed for this purpose populates stars along the isochrone according to the timescales predicted by the models. We know that the observed cluster CMDs have scatter around the actual evolutionary path, and as the synthetic CMD as well as the integrated luminosity function (ILF) was used to compare with the observed ones, the factors that produce scatter in

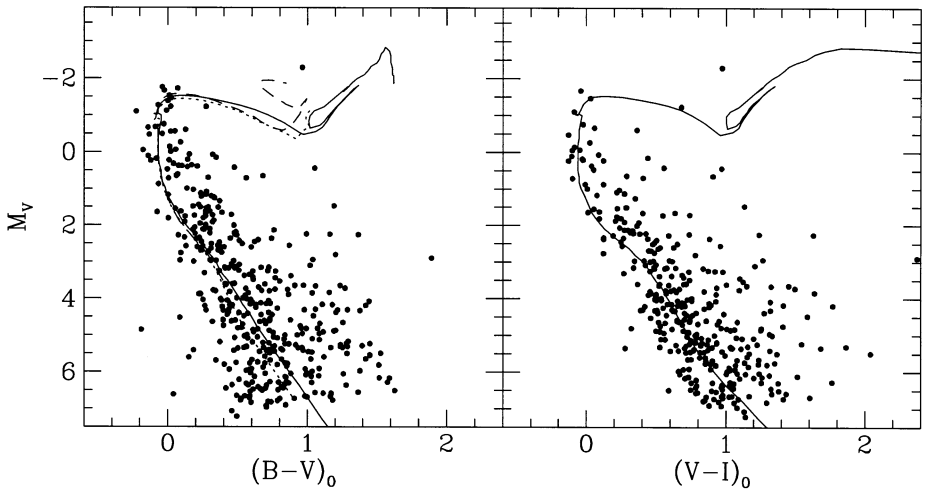

FIG. 27.—Isochrones are plotted to match the CMDs of the cluster NGC 1912; see Fig. 26 for details

TABLE 10

AGE (log τ) OF THE FIVE OPEN CLUSTERS AS ESTIMATED FROM THE THREE MODELS

	log τ				
MODEL	NGC 1907	NGC 1912	NGC 2383	NGC 2384	NGC 6709
1	8.45	8.2	8.45	7.1	8.35
2	8.6	8.4	8.6	7.2	8.5
3	8.6	8.4	8.6	7.3	8.5

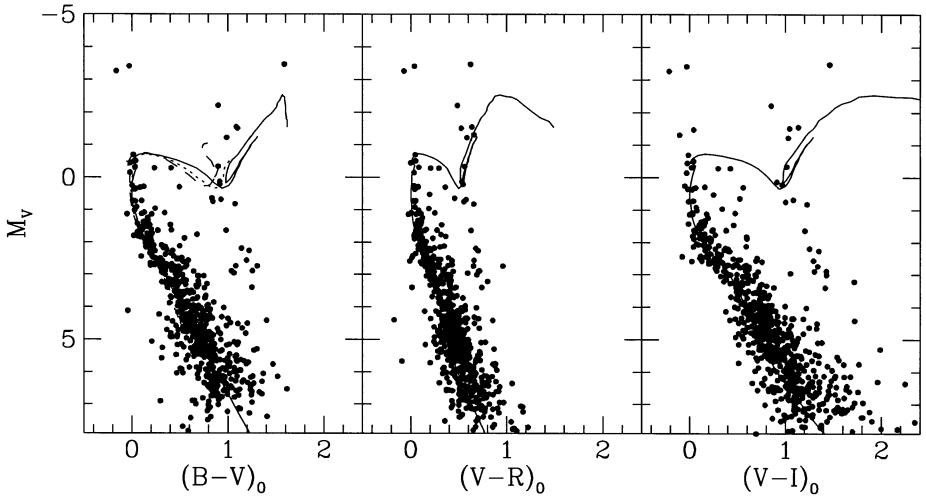

FIG. 28.—Isochrones are plotted to match the CMDs of the cluster NGC 2383; see Fig. 26 for details

the MS as well as in the evolved region of the cluster CMDs have to be incorporated. The two main factors considered here are the binary stars in the cluster and the observational photometric errors. The presence of binaries in a cluster produces width in the MS and scatter near the turn-off and in all the later evolutionary stages. The attempts to find the percentage of spectroscopic binary stars in open clusters indicate that it varies between 30%–50% (Mermilliod &

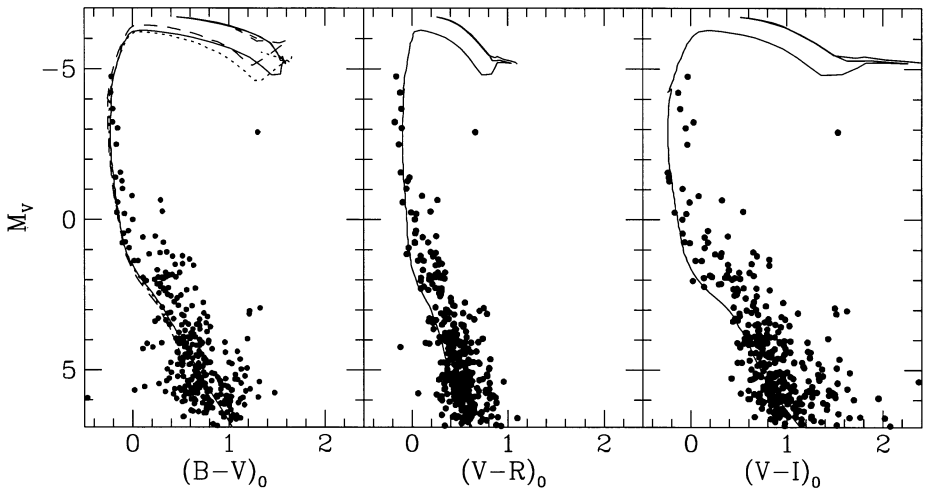

FIG. 29.—Isochrones are plotted to match the CMDs of the cluster NGC 2384; see Fig. 26 for details

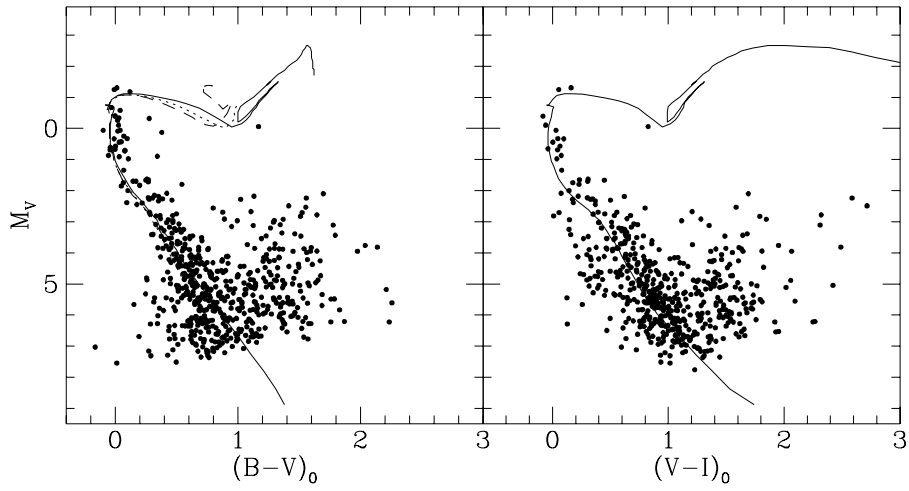

FIG. 30.—Isochrones are plotted to match the CMDs of the cluster NGC 6709; see Fig. 26 for details

Mayor 1989; Crampton, Hill, & Fisher 1976). Therefore, we assume around 30% binaries for computing the synthetic CMD. The effect of binarity in the CMD is at maximum when the ratio of their masses is close to 1, and therefore the mass ratio was chosen to be in the range of 0.75–1.25. The details of the algorithm can be seen in Subramaniam & Sagar (1995).

The synthetic CMDs were obtained using three stellar evolutionary models discussed above. The number of stars in the brighter part of the MS is used for fixing the proportionality constant in the mass function. The number of evolved stars were not used because their number is very small. We first compare the features in the CMDs as predicted by the models with the observed ones and then the ILFs.

10.1. *Comparison of Features*

A comparison between the observed and the synthetic CMDs will help in identifying the model that reproduces evolutionary track closest to the observed one. We take a look at the individual clusters below.

NGC 1907.—This cluster seems to have a decent number of red giants. There are six candidate red giants in the cluster, but no kinematic information is available on their membership. The synthetic CMDs using models 2 and 3 produce the red giant clump, and in the case of model 1, the stars are rather scattered near the clump. Another feature is that model 1 tries to produce stars in the subgiant phase and in the inert helium-core phase, which were not observed. The observed width of the MS (excluding the wide scatter) can be reproduced when the observed photometric error and $\sim 30\%$ binaries are included in the input for the synthetic CMD.

NGC 1912.—This cluster has one red giant star and one star in the subgiant phase. All three models seem to produce more number of red giants when the Salpeter value is used for the mass function slope. Model 1 produces three stars in the evolved phase for $x = 2.0$ and models 2 and 3 produce two and three stars each for $x = 1.7$ (Salpeter value of $x = 1.35$). There are about nine stars seen at the top of the observed MS that lie along the isochrone. None of the models have been able to produce these stars. These lie in the fast evolutionary phase of the isochrone. These stars may be contact binaries or blue straggler candidates.

NGC 2383.—This cluster has a red giant clump consisting of three stars and a subgiant branch with two stars. These can be considered as members. As seen in the case of NGC 1907, the clump is not well reproduced by model 1. Model 2 produces a small amount of scatter in the clump, but model 3 produces a very compact clump. Models 1 and 2 produce one subgiant star, whereas no subgiants are produced by model 3. The required number of stars seen at the top of the observed MS is not obtained in any of the synthetic CMDs, only lesser number of stars are produced. The approximate number of stars in the clump are produced for the Salpeter value of x.

NGC 2384.—This cluster is the youngest among the open clusters studied here. When the value of age as estimated by the isochrone fitting is used to make the synthetic CMDs, the stars at the top of the MS are not populated. We tried to populate them by lowering the age of the cluster. The synthetic CMDs were made using model 2 for an age of 3.2 Myr and $x = 1.0$, model 3 for an age of 8 Myr and $x = 0.8$, and model 1 for an age of 3.2 Myr and $x = 1.0$. Though a few stars are seen in the CMDs using models 1 and 2, the CMD using model 3 populates almost the observed number of stars. Thus, the cluster is younger in age and seems to have a shallower slope for the mass function.

NGC 6709.—This cluster has only one candidate for red giant, which we consider as a member. The synthetic CMDs were constructed with values of x steeper than the Salpeter value of x. Models 1 and 3 put four stars in the evolved phase for $x = 2.0$, whereas model 2 puts two stars for a value of $x = 1.7$. Therefore, the cluster has a steeper value of x compared to the Salpeter value. Again the three stars seen at the top of the observed MS is not generated in the synthetic CMDs.

The synthetic CMDs that closely reproduce the observed features are shown in Figures 31 and 32. The model used to construct the CMD is shown along with the name of the cluster. In general, the evolved parts of the CMDs are better reproduced by models 2 and 3, which include the effects due to core overshoot. The stars that are seen at the top of the cluster MS are not populated in the synthetic CMDs. One star among this group in NGC 1912 was observed spectroscopically and showed giant nature. This may indicate that these stars are in the normal phase of evolution, and hence the evolutionary timescales need to be corrected to produce stars in this region. The nature of the rest of the stars also have to be confirmed. Another possibility is that some of these stars may be contact binaries and blue straggler candidates, in which case they are not in the normal evolutionary phase.

10.2. *Comparison of ILFs*

Chiosi et al. (1989) showed that the ILF of MS stars normalized to the number of evolved stars can be used to differentiate among different evolutionary scenarios, since it is just the ratio of core H- to He-burning lifetimes that is very much affected by the mixing scheme used. Here we compare the observed ILFs of MS, normalized to the number of evolved stars with those estimated from the synthetic CMDs. This is not attempted in the case of NGC 1907, as the estimates of field star contamination are not available.

The synthetic CMDs were constructed for varying values of the MF slope, x, and the ILFs are calculated in each case. The results for the four clusters are shown in Figure 33 and are tabulated in Table 11. The values of the percentage of binary stars used are also given in the table.

The ILF of NGC 1912 is best matched by the ILF computed from model 2, with a slope $x = 1.7$. The ILFs computed from models 1 and 3 computed with $x = 2.0$ follow closely, within the error of the observed ILF. Though the distinction between the ILFs computed from different models is not much, model 2 ought to be preferred. Also, the cluster mass function slope seems to be 1.7, which is steeper than the Salpeter value. In the case of NGC 2383, the ILFs from all three models come close to the observed one for a value of 1.3 for x. The ILF computed from model 1 deviates at the fainter limits, and the ILFs from models 2 and 3 are very similar. The distinction between the overshoot models is not possible in this case, but the overshoot models have to be preferred. The cluster mass function is similar to the Salpeter value of 1.35. The age of the cluster NGC 2384 from the synthetic CMD is much lower than that obtained from the isochrone fit. Also, in order to populate the brightest part of the MS, a shallower value of x is used. Models 1

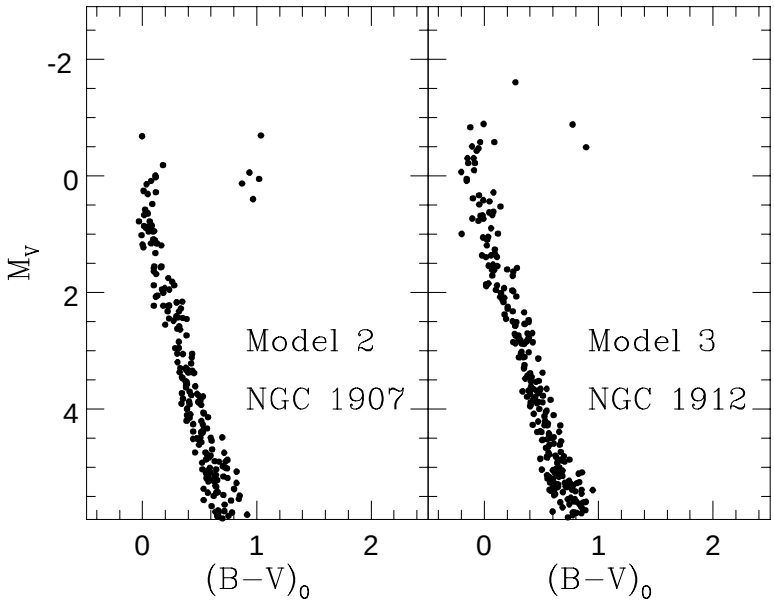

FIG. 31.—Synthetic CMDs that reproduce the observed features are shown here. The model used to produce the synthetic CMD is shown.

and 2 are not able to produce a synthetic CMD close to the observed one, in the brighter end. The synthetic ILFs from all three models match in the fainter end of the observed ILF. The mass function slope for the cluster is 1.0, which is shallower than the Salpeter value. For the cluster NGC 6709, the observed ILF matches the ILF computed from model 2. The other two models do not come close even within the error. The important point to be noted here is that, the number of evolved stars observed is one, and hence the observed ILF is normalized using this number. The

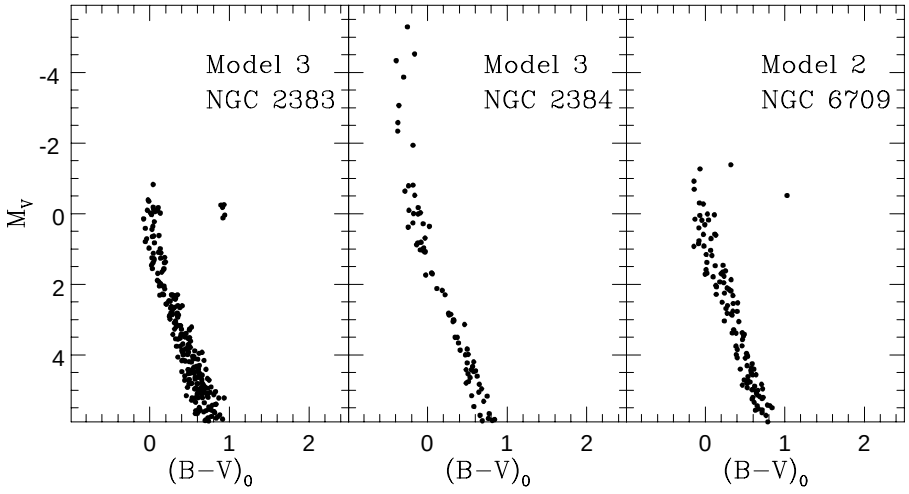

FIG. 32.—Synthetic CMDs that reproduce the observed features are shown here. The model used to produce the synthetic CMD is shown.

TABLE 11

VALUES OF x AND PERCENTAGE OF BINARY

		MODEL 1		MODEL 2		MODEL 3	
CLUSTER	MASS RANGE	x	Binary	x	Binary	x	Binary
NGC 1912.....	3.9–1.7	2.0	30	1.7	30	2.0	30
NGC 2383.....	3.1–1.7	1.3	20	1.3	30	1.3	25
NGC 2384.....	14.0–2.0	1.0	0	1.0	0	0.8	0
NGC 6709.....	3.4–1.7	2.0	20	1.7	45	2.0	35

NOTE.—Values of x and percentage of binary are tabulated here, which are used as inputs to construct the synthetic ILFs shown in Fig. 31.

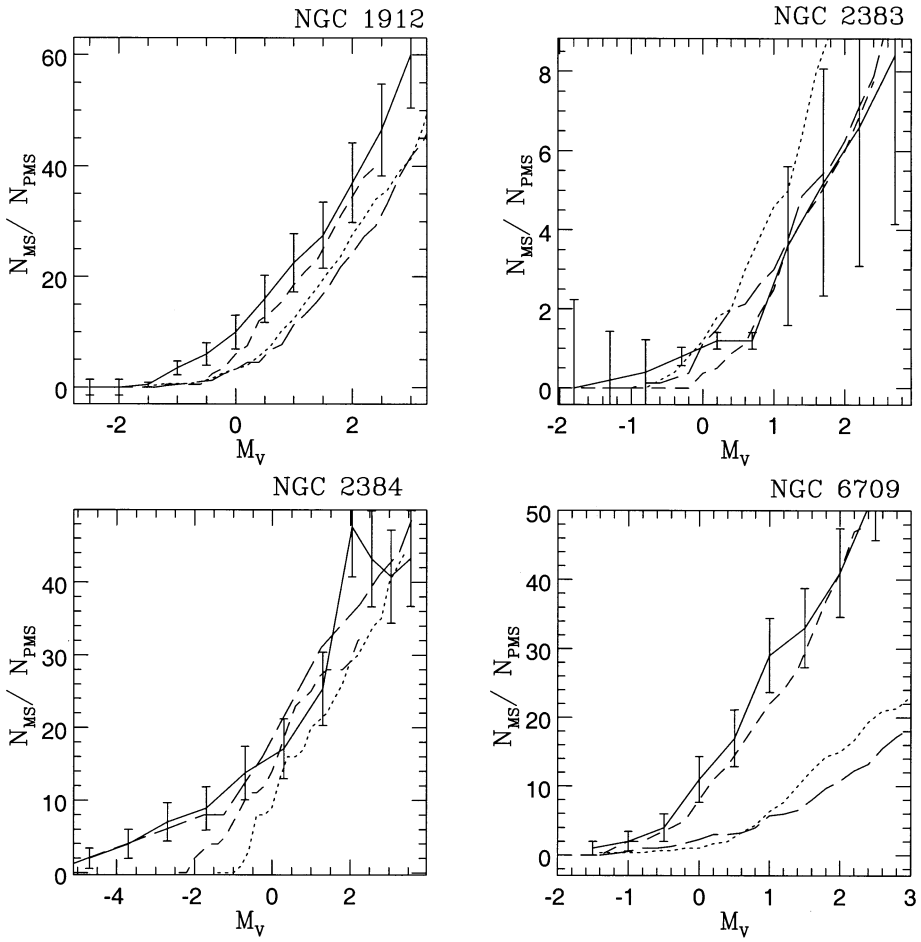

FIG. 33.—Synthetic ILFs are compared with the observed ILFs. The solid line is the observed one, model 1 is the dotted line, model 2 is the short-dashed line, and model 3 is the long-dashed line. The details of the synthetic CMDs used to calculate the plotted ILFs are tabulated in Table 11.

statistical error is equal to the value itself, and this can make the ILFs of all three models agree with the observed ones within errors. The mass function used for model 2 is 1.7, with still steeper values for the other two models. The cluster mass function is thus $x = 1.7$. The error involved in estimating the slope of the mass function, x is ~ 0.15.

The results obtained from the comparison of the ILFs can be directly converted to the comparison of the ratio of the evolutionary timescales. The turn-off mass of the clusters corresponding to the age estimated from the models are tabulated in Table 12. The ratio of the helium core burning to hydrogen core burning lifetimes corresponding to these masses are also tabulated.

It can be seen that the cluster ages estimated using the classical model, model 1 is younger and the turn-off mass, M_{TO}, heavier than the overshoot models. Though the two overshoot models, models 2 and 3 estimate the same ages for the older clusters, the M_{TO} given by model 2 is lighter than that given by model 3. Also, the value of the lifetime ratio τ_{He}/τ_H is smaller in the case of model 2 compared to model 3. The comparison of ILFs show that model 2 is to be preferred marginally to model 3. This may indicate that the smaller of the two lifetime ratios presented by the overshoot models is to be preferred.

As seen above, the number of stars observed in the evolved phase of the cluster CMD is much lower, in order

TABLE 12

TURN-OFF MASSES FOR THE CLUSTERS AS OBTAINED FROM THE THREE MODELS

	MODEL 1		MODEL 2		MODEL 3	
CLUSTER	M_{TO}	τ_{He}/τ_H	M_{TO}	τ_{He}/τ_H	M_{TO}	τ_{He}/τ_H
NGC 1912.....	3.9	0.321	3.35	0.210	3.5	0.225
NGC 2383.....	3.15	0.390	2.8	0.246	2.9	0.297
NGC 2384.....	14.34	...	11.6	0.098	11.3	0.062
NGC 6709.....	3.4	0.379	3.0	0.245	3.2	0.262

NOTE.—The lifetime ratio τ_{He}/τ_H corresponding to the masses are also tabulated.

to make the results statistically significant. The errors in the observed ILFs can be reduced if the number of stars in the evolved phase is high. This can be achieved by using the CMDs of populous clusters in the LMC (Subramaniam & Sagar 1995).

11. CANDIDACY OF THE TWO DOUBLE CLUSTERS

NGC 1907 + NGC 1912.—The clusters NGC 1907 + NGC 1912 lie in the constellation of Auriga. We estimated the distance to the clusters to be 1785 ± 80 pc for NGC 1907 and 1810 ± 80 for NGC 1912. With the new distance, the separation between the clusters become 18.8 pc. There is a difference of 0.12 mag in reddening between these two clusters, primarily because of the foreground Taurus-Auriga cloud, which gives rise to differential reddening in this direction. This is evident from the cluster region as seen in the Palomar chart. The present age estimates show that the two clusters have similar ages. The age estimated using Bertelli et al. (1994) isochrones are 4×10^8 and 2.50×10^8 yr for NGC 1907 and NGC 1912, respectively. Available metallicity estimates find similar values for the clusters. The radial velocity determination of these two clusters by Glushkova & Rastorguev (1991) found that these clusters have very similar radial velocity. These facts strengthen the argument that the two clusters might be born from the same cloud nearly at the same time.

NGC 2383 + NGC 2384.—These two clusters lie in the constellation of Canis Major. Vogt & Moffat (1972) commented on these two clusters and found that they lie in two different arms and they are close in the sky, just because of projection. The present analysis finds that NGC 2383 and NGC 2384 lie close to each other, at a distance of 3340 ± 155 and 2935 ± 135 pc, respectively. The separation between the clusters now becomes 9.2 pc. The reddening values are very similar. The radial velocity estimate is available only for NGC 2384, and metallicity estimates are not available for both the clusters. The present age estimates show that these two clusters have different ages. The ages estimated using Bertelli et al. (1994) isochrones are 4×10^8 yr for NGC 2383 and 2×10^7 yr for NGC 2384. This indicates that these clusters are not born together.

The open clusters in the Galaxy are distributed close to the Galactic plane with a scale height of only 70 pc. They are hence subjected to a strong tidal field due to differential rotation in the Galaxy. The lifetime of a cluster is in fact determined by the tidal field and is disrupted typically after a few 10^8 yr. The influence of the Galactic tidal field is stronger on the binary/double cluster due to its larger extent and could potentially disrupt the pair in its early stages, and the pair may not remain bound for even a fraction of the cluster lifetime. The tidal disruption times for these two candidate cluster pairs have been estimated as explained in Subramaniam et al. (1995). With the new distance estimates for the two pairs, NGC 1907 + NGC 1912 and NGC 2383 + NGC 2384, the tidal disruption timescale, $\log t_{\rm tidal}$ becomes 7.0 and 8.36, respectively.

12. DISCUSSION AND CONCLUSIONS

The results of the distance and reddening determinations of the five clusters, NGC 1907, NGC 1912, NGC 2383, NGC 2384, and NGC 6709, are presented here. All the distances obtained here are larger than those given in Lyngå (1987) catalog. The present distances are larger by 35%, 25%, 65%, 45%, and 30% in the case of NGC 1912, NGC 6709, NGC 2383, NGC 2384, and NGC 1907, respectively. The present determinations are based on more number of stars in a wider range of brightness and are estimated with the help of the cluster CMDs not only in the V versus $B-V$ plane but also in V versus $V-I$ and V versus $V-R$ in two cases. Therefore, the present estimates can be considered as more accurate. On the other hand, the $E(B-V)$ reddening values are the same within errors, except in the case of NGC 6709, where the present reddening is less by 0.1 mag.

The reddening toward the clusters are determined from the photometry using two methods. The $E(B-V)$ values determined using the method of Natali et al. (1994) give values similar to the ones obtained from ZAMS fitting method, except in the case of NGC 6709. In the case of NGC 6709, the second method estimates a reddening larger by 0.15 mag when compared to the first one. As explained earlier, this method seems to determine the reddening toward the Galactic field rather than toward the cluster.

From the spectra obtained in this study we could identify two stars with Hα emission. One star is in NGC 6709 (star S2a), which is already known to have Hα emission, and the other one is in NGC 2383 (star S10), which has been identified for the first time. The present resolution does not show any shell feature for the star S2a, as mentioned by Sowell (1987). The Hβ profile of the star S10 shows a shell feature in one spectra that needs to be confirmed. The CMDs of NGC 1912 show a large amount of spread in the $B-V$ color. This may be due to the presence of a large fraction of binaries, fast rotating stars or peculiar stars as seen in the case of NGC 2287 (Harris et al. 1993). Spectra of more stars in this cluster with better resolution are needed to identify the peculiar stars, if any.

We have compared the CMDs and LFs derived from a homogeneous set of data comprising of four open clusters with turn-off masses in the range 2.8–4.0 $M_\odot$ and $\sim 12\, M_\odot$ with the synthetic ones produced using the stellar evolutionary models from Castellani et al. (1990), Schaller et al. (1992), and Bressan et al. (1993). Therefore, this study covers the range of intermediate- to high-mass stars.

Two of the old open clusters, NGC 1912 and NGC 6709, show clumpiness in the MS of their CMD. The reason for this is not known. It is important to know the reason as most of the stars in these cluster MS happen to lie in the clumps. More photometric and spectroscopic observation of some stars in these clumps are needed to find presence of high rotation or spots etc., which might help in understanding the nature of these stars. In the case of open clusters the stars seen at the very bright end of the MS were not populated in the synthetic CMDs of classical as well as the overshoot models. This was noticed also in the case of LMC clusters (Subramaniam & Sagar 1995). If these stars are in the normal evolutionary phase, then the evolutionary timescale have to be modified to populate stars in this region. More observations are needed to identify the nature of these stars—whether they are peculiar stars like accreting binaries, etc.

Subramaniam et al. (1995) have classified NGC 1907 and NGC 1912 as a probable double cluster. From the present determinations of the cluster parameters it can be seen that these clusters have similar values for distance and age. Therefore, the present result strengthens the candidacy of NGC 1907 + NGC 1912 for a binary cluster, with common

origin. The tidal timescale for this pair is less than their age, which might indicate that the clusters are not gravitationally bound. Another pair, NGC 2383 + NGC 2384 listed by Subramaniam et al. (1995) also has similar values for their distances and therefore lie close to each other in space. But this pair cannot have common origin as the present age estimates show that NGC 2383 is an intermediate-age cluster, whereas NGC 2384 is a very young cluster.

Between Galactic latitudes $231° \leq l \leq 256°$, the interstellar absorption is small up to large distances. The reddening increases slowly to a distance of 1 kpc, and beyond that it is nearly a constant reddening [$E(B-V) = 0.3$ mag] out to more than 4 kpc (Isserstedt & Schmidt-Kaler 1964; Neckel & Klare 1980). This implies that nearly all reddening between 1 and 4 kpc is caused by local dust clouds lying within 1 kpc (see Vogt & Moffat 1972). In the present study, the clusters NGC 2383 and NGC 2384 lie in this region. We find the reddening to be 0.25 mag on an average to a distance of ~ 3 kpc, which supports the above statement.

In general, the features of the observed CMDs are well reproduced by overshoot models. In the lower mass range considered, the distinction between the two overshoot models could not be made. Model 3 is preferred to model 2 in the case of the higher mass range. As far as the lifetime ratios are concerned, a clear-cut picture does not emerge from the present analysis. The analysis of the LMC clusters showed that the fine tuning of the percentage of binary stars and the slope of mass function can bring the synthetic ILFs of all the models to match the observed ILFs. This procedure is not attempted in the case of open clusters because of the poor number statistics. Though model 2 seems to have the value of τ_{He}/τ_H close to the observed one, the statistical uncertainty pushes the values of the other two models also within the errors of the observed one.

The mass functions for the clusters were determined using comparison of ILF. The values obtained as shown in Table 11 show that the clusters NGC 1912 and NGC 6709 have the same slope for the mass function (1.7 ± 0.15) in the mass range 1.7–3.9 $M_\odot$ and 1.7–3.4 $M_\odot$, respectively. This is a slightly higher value in comparison to the Salpeter value of 1.35. The cluster NGC 2383 has slope (1.3 ± 0.15) in the mass range 1.7–3.1 $M_\odot$, which is very similar to the Salpeter value. On the other hand, the cluster NGC 2384 has a lower value for the mass function slope (1.0 ± 0.15) in the mass range 2.0–14.0 $M_\odot$. This indicates that this cluster may be deficient in low-mass stars, as seen from the cluster CMDs. A similar case is noticed by Phelps & Janes (1993) for NGC 663. They found a slope of 1.06 ± 0.05 in the mass range 1.4–12.0 $M_\odot$. In the case of NGC 3293, Herbst & Miller (1982) found a slope of 0.8 ± 0.2. They also found a deficiency of low-mass stars in this cluster. The other recent estimates of mass function slopes were made by Moitinho et al. (1997), and Forbes (1996), and they found the slopes to be similar to the Salpeter value. Phelps & Janes (1993) also found Salpeter slope for most of the clusters analyzed by them.

Another point to be noticed is that, for ages of more than 10^8 yr, models 2 and 3 estimate similar ages, whereas for younger clusters, model 2 estimates a younger age when compared with model 3. For old clusters, when models 2 and 3 estimate similar ages, model 2 estimates a lower turn-off mass and τ_{He}/τ_H ratio compared to model 3. In the case of younger (LMC) clusters, model 3 has the lower M_{TO} and τ_{He}/τ_H. Though the models use the same amount of core overshooting, they seem to differ in the lower and the higher mass ranges considered.

The main results of the present investigation are the following: We present new estimates of reddening, distance, and age for five open clusters of our Galaxy. We also present the results spectral classification for 47 bright members of these clusters, except NGC 1907. In the cluster NGC 2383, we found an Hα emission star for the first time. The CMDs of these clusters are presented identifying the probable members in the brighter part of the CMDs. The present distance estimates are seen to be larger than those in the Lyngå (1987) catalog, while the estimated values of reddening are similar. Some gaps in the cluster main sequence have been identified. The age of the clusters estimated using the isochrones of Bertelli et al. (1994) are 400, 250, 400, 20, and 315 Myr for the clusters NGC 1907, NGC 1912, NGC 2383, NGC 2384, and NGC 6709. Analysis using synthetic CMDs shows that classical models make the clusters younger but the turn-off masses slightly heavier in comparison to the models incorporating the overshooting of the convective core. In general, the overshoot models reproduce the observed features when compared to the classical models. The synthetic ILF derived from a model strongly depends on the value of the mass function slope and lightly on the binary fraction, whereas the observed ILFs are affected by the uncertainty in the number of evolved stars. Hence, the comparison of the synthetic with the observed ILFs does not favor any model specifically (see Fig. 33). In order to differentiate among the models from the comparison of the synthetic ILFs with the observed ones, reliable estimates of mass function slope, binary fraction are desired. The ILF comparison can limit the values of the mass function slopes to a certain extent. The values of the mass function slopes are as follows: NGC 1912 and NGC 6709 have $x = 1.7 \pm 0.15$, NGC 2383 has $x = 1.3 \pm 0.15$, and NGC 2384 has $x = 1.0 \pm 0.15$. We find that the double cluster NGC 1912 + NGC 1907 have similar distances and ages, indicating that they may have born together making this a good candidate for a binary open cluster.

This research has made use of the SIMBAD database, operated at CDS, Strasbourg, France. We thank J.-C. Mermilliod for providing us with a copy of the open cluster database.

REFERENCES

Alongi, M., Bertelli, G., Bressan, A., Chiosi, C., Fagotto, F., Greggio, L., & Nasi, E. 1993, A&AS, 97, 851
Anthony-Twarog, B. J., Heim, E. A., Twarog, B. A., & Caldwell, N. 1991, AJ, 102, 1056
Aparicio, A., Alfaro, E. J., Delgado, A. J., Rodriguez-Ulloa, J. A., & Cabrera-Cano, J. 1993, AJ, 106, 1547
Aparicio, A., Bertelli, G., Chiosi, C., & Garcia-Pelayo, J. M. 1990, A&A, 240, 262
Babu, G. S. D. 1985, Ph.D. thesis, Indian Inst. Astrophys.
Becker, W. 1963, Z. Astrophys., 57, 117
Bergbusch, P. A., VandenBerg, D. A., & Infante, L. 1991, AJ, 101, 6
Bertelli, G., Bressan, A., & Chiosi, C. 1992, ApJ, 392, 522
Bertelli, G., Bressan, A., Chiosi, C., & Angerer, K. 1986a, A&AS, 66, 191
———. 1986b, Mem. Soc. Astron. Italiana, 57, 427
Bertelli, G., Bressan, A., Chiosi, C., Fagotto, F., & Nasi, E. 1994, A&AS, 106, 275
Bertelli, G., Bressan, A., Chiosi, C., Mateo, M., & Wood, P. R. 1993, ApJ, 412, 160

Böhm-Vitense, E., & Canterna, R. 1974, ApJ, 194, 629
Breger, M. 1976, ApJS, 32, 7
Bressan, A., Fagotto, F., Bertelli, G., & Chiosi, C. 1993, A&AS, 100, 647
Carraro, G., Chiosi, C., Bressan, A., & Bertelli, G. 1994, A&AS, 103, 375
Castellani, V., Chieffi, A., & Straniero, O. 1990, ApJS, 74, 463
———. 1992, ApJS, 78, 517
Chevalier, C., & Ilovaisky, S. A. 1991, ApJS, 90, 225
Chiosi, C., Bertelli, G., Meylan, G., & Ortolani, S. 1989, A&A, 219, 167
Collinder, P. 1931, Ann. Lund. Obs., 2
Crampton, D., Hill, G., & Fisher, W. A. 1976, ApJ, 204, 502
Fitzgerald, M. P., Luiken, M., Maitzen, H. M., & Moffat, A. F. J. 1979, A&AS, 37, 345
Forbes, D. 1996, AJ, 112, 1073
Glushkova, E. V., & Rasorguev, A. S. 1991, Soviet Astron. Lett., 17, 13
Hakkila, J., Sanders, W. L., & Schroder, R. 1983, A&AS, 51, 541
Harris, G. L. H., Fitzgerald, M. P. V., Mehta, S., & Reed, B. C. 1993, AJ, 106, 1533
Hassan, S. M. 1984, in Astronomy with Schmidt-Type Telescope, (Dordrecht: Reidel), 295
Hawarden, T. G. 1971, Observatory, 91, 78
Hayford, P. 1932, Lick. Obs. Bull., 16, 53
Herbst, W., & Miller, D. P. 1982, AJ, 87, 1478
Hiltner, W. A. 1956, ApJS, 2, 389
Hoag, A. A. 1966, Vistas Astron., 8, 139
Hoag, A. A., & Applequist, L. 1965, ApJS, 12, 215
Hoag, A. A., Johnson, H. L., Iriarte, B., Mitchell, R. I., Hallam, K. L., & Sharpless, S. 1961, Publ. US Naval. Obs., 17, 347
Hron, J., Maitzen, H. M., Moffat, A. F. J., Schmidt-Kaler, T., & Vogt, N. 1985, A&AS, 60, 355
Huebener, W. F., Merts, A. L., Magu, N. H., & Agro, M. F. 1977, Los Alamos Sci. Lab. Rep. LA-6760-M
Isserstedt, J., & Schmidt-Kaler, T. 1964, Z. Astrophys., 59, 182
Jacoby, G. M., Hunter, D. A., & Christian, C. A. 1984, ApJS, 56, 257
Jeffers, H. M., van den Bos, W. H., & Greeby, F. M. 1963, Publ. Lick Obs., 21
Johnson, H. L. 1961, Lowell Obs. Bull., 5, N8
———. 1966, ARA&A, 4, 193
Joner, M. D., & Taylor, B. J. 1990, PASP, 102, 1004
Kjeldsen, K., & Frandsen, S. 1991, A&AS, 87
Kurucz, R. L. 1979, ApJS, 40, 1
Liu, T., Janes, K. A., & Bania, T. M. 1989, AJ, 98, 626
———. 1991, ApJ, 377, 141
Lyngå, G. 1987, Calalog of Open Star Cluster Data (Strasbourg: CDS)
Maeder, A., & Mermilliod, J.-C. 1981, A&A, 93, 136
Maeder, A., & Meynet, G. 1989, A&A, 210, 155
———. 1991, A&AS, 89, 451
Mateo, M. 1988, ApJ, 331, 281
Mermilliod, J.-C. 1976, A&A, 53, 289
———. 1994, Calalog of Open Cluster Data (Strasbourg: CDS)
Mermilliod, J.-C., & Mayor, M. 1989, A&A, 288, 618
Mills, G. A. 1967, J. Obs., 50, 179
Moitinho, A., Alfaro, E. J., Yun, J. L., & Phelps, R. L. 1997, AJ, 113, 1359
Montgomery, A. S., Marschall, L. A., & Janes, K. A. 1993, AJ, 106, 181
Natali, F., Natali, G., Pompei, E., & Pedichini, F. 1994, A&A, 289, 756
Neckel, Th., & Klare, G. 1980, A&AS, 42, 251
Phelps, R. L., & Janes, K. A. 1993, AJ, 106, 1870
———. 1994, ApJS, 90, 31
Sagar, R., & Griffiths, W. K. 1998, MNRAS, 299, 777
Sagar, R., & Pati, A. K. 1989, Bull. Astron. Soc. India, 17, 6
Sagar, R., & Richtler, T. 1991, A&A, 250, 324
Sagar, R., Richtler, T., & de Boer, K. S. 1991, A&AS, 90, 387
Schaller, G., Schearer, D., Meynet, G., & Maeder, A. 1992, A&AS, 96, 269
Schild, R. E. 1983, PASP, 95, 1021
Schild, R. E., & Romanishin, W. 1976, ApJ, 204, 493
Schmidt-Kaler, T. 1982, in Landolt-Börnstein, Group VI, Vol. 2b, Stars and Star Clusters (Berlin: Springer)
Sears, R. L., & Sowell, J. R. 1997, AJ, 113, 1039
Sowell, J. R. 1987, ApJS, 64, 241
Stetson, P. B. 1987, PASP, 99, 191
———. 1992, in IAU Colloq. 136, Stellar Photometry—Current Techniques and Future Developments, ed. C. J. Butler & I. Elliott (Cambridge: Cambridge Univ. Press), 291
Strobel, A. 1991, ApJ, 376, 204
Subramaniam, A., Gorti, U., Sagar, R., & Bhatt, H. C. 1995, A&A, 302, 86
Subramaniam, A., & Sagar, R. 1995, A&A, 297, 695
Trumpler, R. J. 1930, Lick Obs. Bull., 14, 154
VandenBerg, D. A. 1983, ApJS, 51, 29
Vogt, N., & Moffat, A. F. J. 1972, A&AS, 7, 133
Wilner, D. J., & Lada, C. J. 1991, AJ, 102, 1050
Young, A., & Martin, A. E. 1973, ApJ, 181, 805